5-Substituted Derivatives of 6-Halogeno-3-((2-(*S*)-azetidinyl)methoxy)pyridine and 6-Halogeno-3-((2-(*S*)-pyrrolidinyl)methoxy)pyridine with Low Picomolar Affinity for α4*β*2 Nicotinic Acetylcholine Receptor and Wide Range of Lipophilicity: Potential Probes for Imaging with Positron Emission Tomography

Yi Zhang, Olga A. Pavlova, Svetlana I. Chefer, Andrew W. Hall, Varughese Kurian, LaVerne L. Brown, Alane S. Kimes, Alexey G. Mukhin, and Andrew G. Horti*

Neuroimaging Research Branch, Intramural Research Program, National Institute on Drug Abuse, NIH, DHHS, 5500 Nathan Shock Drive, Baltimore, Maryland 21224

Received September 3, 2003

Potential positron emission tomography (PET) ligands with low picomolar affinity at the nicotinic acetylcholine receptor (nAChR) and with lipophilicity (log *D*) ranging from −1.6 to +1.5 have been synthesized. Most members of the series, which are derivatives of 5-substituted-6-halogeno-A-85380, exhibited a higher binding affinity at α4*β*2-nAChRs than epibatidine. An analysis, by molecular modeling, revealed an important role of the orientation of the additional heterocyclic ring on the binding affinity of the ligands with nAChRs. The existing nicotinic pharmacophore models do not accommodate this finding. Two compounds of the series, 6-[^{18}F]-fluoro-5-(pyridin-3-yl)-A-85380 ([^{18}F]**31**) and 6-chloro-3-((2-(*S*)-azetidinyl)methoxy)-5-(2-[^{18}F]-fluoropyridin-5-yl)pyridine) ([^{18}F]**35**), were radiolabeled with ^{18}F. Comparison of PET data for [^{18}F]**31** and 2-[^{18}F]FA shows the influence of lipophilicity on the binding potential. Our recent PET studies with [^{18}F]**35** demonstrated that its binding potential values in Rhesus monkey brain were ca. 2.5 times those of 2-[^{18}F]FA. Therefore, [^{18}F]**35** and several other members of the series, when radiolabeled, will be suitable for quantitative imaging of extrathalamic nAChRs.

Introduction

Cerebral nicotinic acetylcholine receptors (nAChRs) play important roles in various brain functions and pathological states.[1] Nicotine is known to improve learning and memory, suggesting the possibility that nicotine and other nicotinic ligands could be useful as medication for attention deficit hyperactivity disorder.[2] The density of cerebral nAChRs is decreased in neurodegenerative diseases, such as Alzheimer's and Parkinson's diseases,[3,4] and increased in smokers.[5] Recent studies suggested a link between an idiopathic partial epilepsy syndrome and a mutation in the gene coding for the α4 subunit of nAChRs.[6] Also, there is evidence of high incidence of smoking among individuals suffering from schizophrenia, bipolar disorder, and major depression.[7] Postmortem studies of human subjects suffering from these psychopathologic disorders showed an altered density of nAChRs.[7] Furthermore, analgesic properties of nicotine and its agonists have stimulated the pharmaceutical industry to investigate analogues of nicotine as novel analgesics.[8] Currently, positron emission tomography (PET) is one of the most advanced techniques available for noninvasive, in vivo studies of cerebral receptors for the study of normal and pathological brain function and diseases and for drug development research. PET imaging requires an appropriate radioligand labeled with a positron-emitting isotope. As applied to imaging of cerebral nAChRs, PET is still in the early stages of development because of a lack of suitable radioligands. One reason for the delayed development of PET imaging of nAChRs compared to the imaging of many other cerebral receptors is the relatively low density of nAChRs in the brain. Hence, a radioligand with a very high binding affinity is required for PET imaging of nAChRs. One of the two most abundant subtypes of nAChRs in mammalian brain is the receptor containing α4 and *β*2 subunits. Consistent with nomenclature recommended by NC-IUPHAR, this receptor is abbreviated throughout the text as α4*β*2-nAChR.[9] The density value (B_{max}) of the α4*β*2-nAChR is highest in the thalamus (10−60 fmol/mg protein) and lower in the extrathalamic regions such as the cortex (4−21 fmol/mg protein).[10−12] Most cerebral receptors that have been successfully studied by PET (for example, D_1, D_2, *μ*-opiate, and benzodiazepine receptors) display substantially higher densities[13−18] than those of the α4*β*2-nAChR. Because of low density of α4*β*2-nAChR, radioligands with very high binding affinities have been synthesized for PET imaging.[19−23] For imaging extrathalamic α4*β*2-nAChRs, radioligands with even higher binding affinity are necessary.

Another important characteristic of a radioligand suitable for neuroimaging is lipophilicity. It is well understood that an optimally high lipophilicity (log *P* = 0−3) of drugs is required for good blood−brain barrier (BBB) permeability.[24−27] However, a lower lipophilicity is desirable to decrease nonspecific binding of a radio-

* To whom correspondence should be addressed. Phone: +1-410-550-2916. Fax: +1-410-550-2724. E-mail: ahorti@intra.nida.nih.gov.

10.1021/jm030432v
Published on Web 04/06/2004

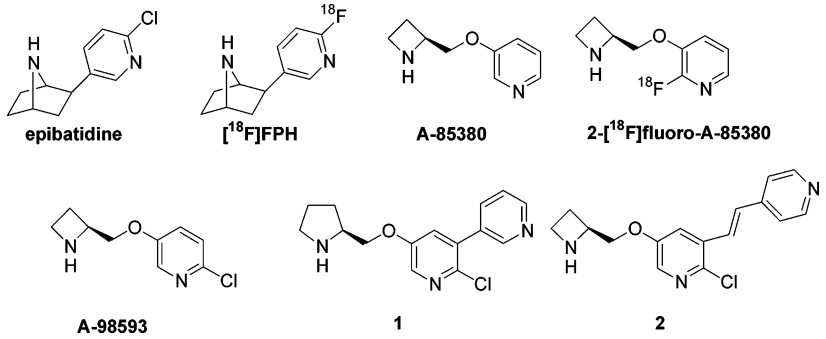

Figure 1. High-affinity nAChR ligands and PET radiotracers.

Table 1. Calculated Apparent and Global Lipophilicity (*c*log $D_{7.4}$ and *c*log *P*, Respectively) and Experimental in Vitro Inhibition Binding Affinity Constants of Compounds **31**−**48** and Representative nAChR Ligands

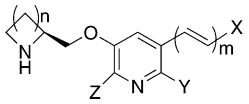

ligand	*m*	*n*	X	Y	Z	*c*log $D_{7.4}$ [a]	*c*log *P*	K_i,[d] pM
Epi[b]	n/a	n/a	n/a	n/a	n/a	−1.27	1.26	9[46]
2-FA[c]	0	1	H	H	F	−1.99[e]	0.45	61 ± 5[38]
A-98593	0	1	H	Cl	H	−1.37	1.15	34[8]
1	0	2	pyridine-3-yl	Cl	H	−0.40	2.06	21[36]
2	1	1	pyridine-4-yl	Cl	H	0.10	2.36	9 ± 1[38]
31	0	1	pyridine-3-yl	F	H	−0.77[e]	1.49	66 ± 2.0 (3)
32	0	1	pyridine-3-yl	Cl	H	−0.93	1.50	8.1 ± 0.8 (3)
33	0	1	pyridine-3-yl	Br	H	−0.65	1.72	6.6 ± 0.8 (4)
34	0	1	pyridine-3-yl	I	H	−0.42	2.06	11.7 ± 1.1 (3)
35	0	1	6-fluoropyridin-3-yl	Cl	H	−0.83[e]	1.49	4.9 ± 0.4 (4)
36	0	1	6-chloropyridin-3-yl	Cl	H	−0.27	2.15	4.5 ± 0.5 (3)
37	0	1	6-bromopyridin-3-yl	Cl	H	−0.14	2.44	4.3 ± 0.3 (3)
38	0	1	5-bromo-6-fluoropyridin-3-yl	Cl	H	−0.12	2.34	4.0 ± 0.5 (3)
39	0	2	6-fluoropyridin-3-yl	Cl	H	−0.32	2.06	17.9 ± 1.6 (3)
40	0	2	6-bromopyridin-3-yl	Cl	H	0.38	3.00	19.5 ± 2.6 (3)
41	0	1	2-fluoropyridin-4-yl	Cl	H	−0.92	1.51	4.8 ± 0.6 (4)
42	0	1	2-bromopyridin-4-yl	Cl	H	−0.23	2.14	3.3 ± 0.4 (3)
43	0	1	6-fluoropyrimidin-3-yl	Cl	H	−1.62	0.82	8.8 ± 0.4 (3)
44	1	1	2-fluoropyridin-4-yl	Cl	H	0.24	2.55	3.1 ± 0.3 (3)
45	1	1	2-bromopyridin-4-yl	Cl	H	0.93	3.23	5.2 ± 0.9 (3)
46	1	2	2-fluoropyridin-4-yl	Cl	H	0.75	3.11	9.4 ± 1.1 (3)
47	1	2	2-bromopyridin-4-yl	Cl	H	1.45	3.79	5.6 ± 0.8 (3)
48	1	1	6-fluoro-5-bromopyridin-3-yl	Cl	H	1.42	3.68	7.7 ± 0.7 (3)

[a] The dissociative partition coefficient (*c*log $D_{7.4}$) and global partition coefficient (*c*log *P*) values were calculated using ACD/LogD Suite software.[49] [b] Epi = Epibatidine. [c] 2-FA = 2-fluoro-A-85380. [d] K_i = mean ± SEM (number of experiments). [e] Experimental log $D_{7.4}$ as determined in four assays (mean ± SD) using the counting technique:[50] 2-[^{18}F]FA (−1.43 ± 0.04); [^{18}F]**31** (−0.82 ± 0.01); [^{18}F]**35** (−0.34 ± 0.01).

ligand.[28] This contradiction often forces researchers to seek a compromise between high BBB permeability and low nonspecific binding or to select radioligands with the lowest lipophilicity within the optimal range.[28−30] Yet, there is no comprehensive understanding of the relationship between lipophilicity and imaging characteristics for many radioligands used for neuroimaging, including those for α4β2-nAChRs. Most PET radioligands that are currently used for imaging a variety of neuroreceptors display lipophilicities within the optimal range for BBB permeability. In contrast, 2-[^{18}F]fluoro-A-85380[22] (Figure 1), the only available PET probe for quantitative imaging of α4β2-nAChRs in humans,[31−33] is a very hydrophilic compound (see Table 1). We suggest that the slow brain kinetics of 2-[^{18}F]fluoro-A-85380 (resulting in long scanning times) may be a consequence of its high polarity. Another limitation of 2-[^{18}F]F-A-85380 is its low binding potential (BP*) values in all regions containing α4β2-nAChRs except the thalamus ($BP^*_{thalamus} \approx 2$).[31,33,34] BP*,[35] a ratio of the volume of distribution of the specific binding compartment to the volume of distribution of the nondisplaceable compartment, characterizes the utility of a radioligand for quantitative imaging of receptors in specified regions. In brain regions with moderate receptor densities such as the cortex and striatum, the BP* of 2-[^{18}F]fluoro-A-85380 is insufficient for quantitative studies (BP* < 0.6 [31,33,34]). The importance of imaging extrathalamic nAChRs has emerged from the demonstration of altered densities of cortical and striatal nAChRs in neurodegenerative diseases.[4] In these disorders, the densities of nAChRs are lower than in control subjects and the BP* values are likely to be correspondingly lower. Higher BP* in these regions can be obtained by radioligands with higher binding affinity.[36−38] However, it is unclear if a radioligand with a higher lipophilicity than that of hydrophilic 2-[^{18}F]-fluoro-A-85380 should be targeted. Currently, there is insufficient data available for nAChR radioligands to determine if the optimal lipophilicity for BBB permeability is also optimal for high binding potential and for faster brain kinetics or vice versa.

Scheme 1[a]

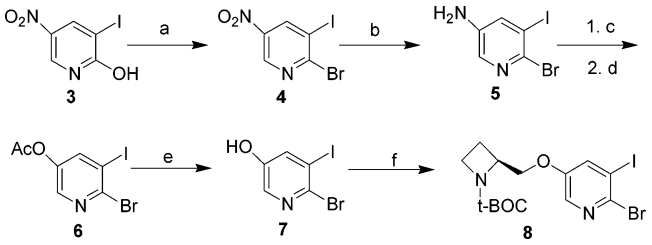

[a] Reagents: (a) $POBr_3$, quinoline, toluene; (b) iron powder, H_2O, AcOH; (c) HBF_4, $NaNO_2/H_2O$; (d) Ac_2O; (e) 2 N KOH, 2-PrOH; (f) 1-(*tert*-butoxycarbonyl)-2(*S*)-azetidinylmethanol, DEAD, PPh_3, toluene.

Scheme 2[a]

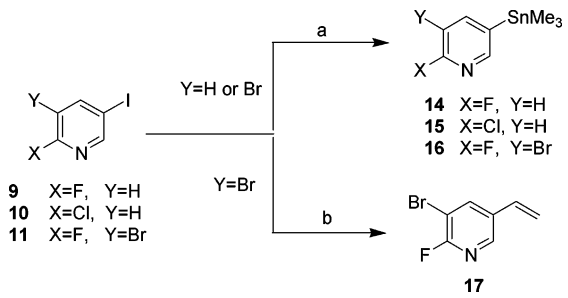

[a] Reagents: (a) $(SnMe_3)_2$, $Pd(PPh_3)_4$/toluene; (b) vinyltributyltin, $Pd(PPh_3)_4$/toluene.

Scheme 3[a]

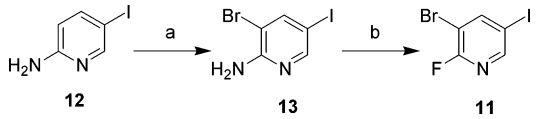

[a] Reagents: (a) NBS, CH_3CN; (b) $NaNO_2$, HF/pyridine.

Therefore, the main goal of the present study is to synthesize a series of ligands for $\alpha4\beta2$-nAChRs exhibiting binding affinities (K_D) in the low picomolar range and a wide range of lipophilicities. The future radiolabeling of the series and evaluation of the radioligands should contribute to our understanding of the influence of lipophilicity on binding potential, BBB permeability, and brain kinetics.

The lead compounds for the series were high-affinity nAChR ligands with moderate lipophilicities: 6-chloro-3-((2-(*S*)-pyrrolidinyl)methoxy)-5-(pyridin-5-yl)pyridine (**1**)[36] and 5-(2-(4-pyridinyl)vinyl)-6-chloro-3-((2-(*S*)-azetidinyl)methoxy)pyridine (**2**)[38] (Figure 1, Table 1).

Results and Discussion

Chemistry. Most compounds in the series (Table 1, **31**−**48**) were prepared via a Stille (Scheme 6) or Heck (Scheme 8) coupling reaction of the iodopyridyl ethers **8**, **27**,[38] and **28**[38] with the corresponding trialkyltin **29**,[39] **14**−**16**, **20**, **21**, **26**, and **30**[40] or vinylheteroarene derivatives **17**, **22**, and **23**, followed by removal of the *t*-BOC protective group. The iodopyridyl ether **8** was synthesized through Mitsunobu coupling of 1-(*tert*-butoxycarbonyl)-2(*S*)-azetidinylmethanol[41] with 2-bromo-3-iodo-5-hydroxypyridine **7** prepared in four steps (Scheme 1).

The trialkyltin heteroaromatic intermediates **14**−**16**, **20**, **21**, and **26** were obtained via palladium-assisted reactions between iodoheteroarene substrates **9**[42]−**11**, **18**,[43,44] **19**, and **25** and hexamethylditin in toluene (Scheme 2, 4, 5). 2-Fluoro-5-trimethyltinpyrimidine **25**

Scheme 4[a]

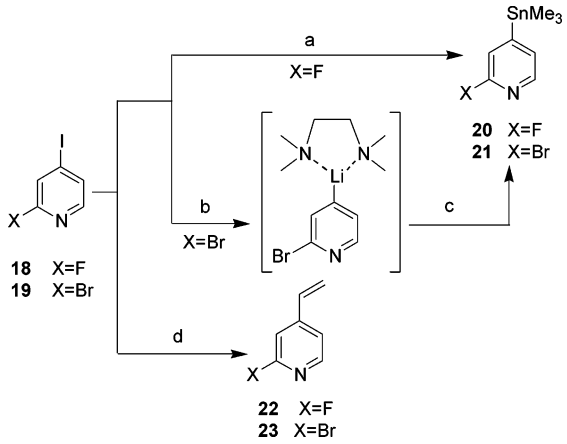

[a] Reagents: (a) hexamethylditin, $Pd(PPh_3)_4$, toluene; (b) *n*-BuLi/*N*,*N*,*N*′,*N*′-tetramethylethylenediamine, ether; (c) $ClSnMe_3$; (d) vinyltributyltin, $Pd(PPh_3)_4$, toluene.

Scheme 5[a]

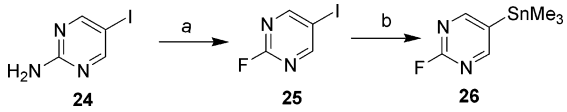

[a] Reagents: (a) $NaNO_2$, HF/pyridine; (b) hexamethylditin, $Pd(PPh_3)_4$, toluene.

was synthesized in two steps through 2-amino-5-iodopyrimidine **24** (Scheme 5). It is noteworthy that the initial attempt to prepare 2-bromo-4-trimethyltinpyridine **21** (Scheme 4) by a conventional palladium-assisted reaction of 2-bromo-4-iodopyridine **19** with hexamethylditin led to a complex mixture of byproducts. The alternative common method of incorporation of the trialkyltin substituent through the corresponding Li−pyridine derivative also failed because metalation of **19** with BuLi followed by treatment with trimethyltin chloride produced only traces of **21**, along with a large amount of impurities. This result may have been due to susceptibility of both halogens and the C−H-(3 or 5) bonds of **19** to metalation and the "halogen-dance".[43] However, the C-(4)-regioselective conversion of **19** to **21** was achieved with a good yield by reaction with BuLi−*N*,*N*,*N*′,*N*′-tetramethylethylenediamine (BuLi*TMEDA) chelate[45] followed by treatment with trimethyltin chloride (Scheme 4). Regioselectivity of the latter reaction can be attributed to altered reactivity of BuLi*TMEDA compared with that of BuLi. This reaction may be the first example of the TMEDA-assisted preparation of a trialkyltinarene derivative.

Vinyl heteroaromatic intermediates **17**, **22**, and **23** were synthesized via a Pd-assisted reaction between iodo-derivatives **11**, **18**, and **19** and tributylvinyltin (Schemes 2 and 4). Intermediate 2-fluoro-3-bromo-5-iodopyridine (**11**) was prepared by bromination of 2-amino-5-iodopyridine (**12**) with *N*-bromosuccinimide followed by deazotization−fluorination of 2-amino-3-bromo-5-iodopyridine (**13**) with sodium nitrite in HF−pyridine solution (Scheme 3). The fluorinated analogue, **31**, was obtained via bromo-to-fluoro exchange reaction of the corresponding bromo-derivative **33a** with anhydrous tetrabutylammonium fluoride followed by *t*-BOC protective group removal (Scheme 7). Similarly, the iodinated analogue, **34**, was obtained via bromo-to-iodo exchange reaction of the corresponding bromo-derivative

Scheme 6[a]

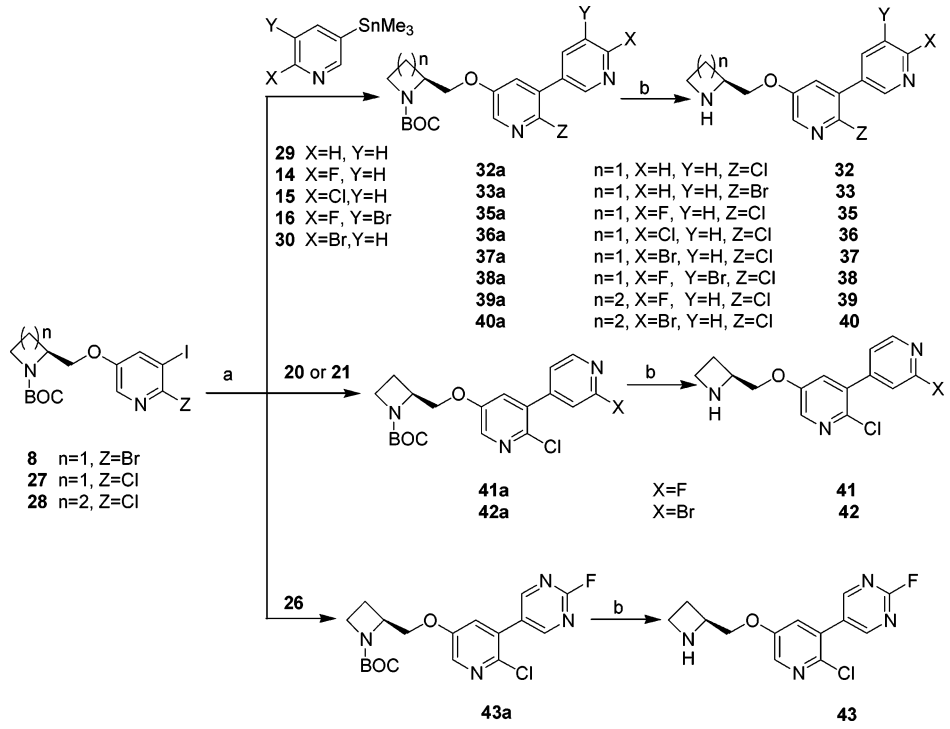

[a] Reagents: (a) $(PPh_3)_4Pd$, toluene; (b) TFA.

Scheme 7[a]

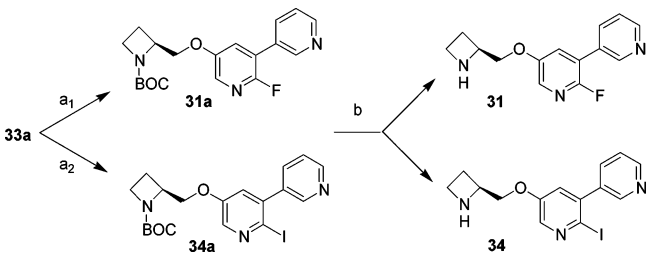

[a] Reagents: (a_1) n-$Bu_4N^+F^-$/DMSO; (a_2) CuI, KI/DMSO; (b) TFA.

33a with a mixture of copper(I) iodide and potassium iodide in anhydrous DMSO solution followed by deprotection (Scheme 7).

In Vitro Binding Assay. The binding affinities for nAChRs of all ligands in the series were determined as described previously[46] by measuring their ability to compete with 50 pM of 5-[^{125}I]iodo-A-85380 for receptor binding sites in rat brain membranes at room temperature. All studied ligands, **31**−**48** (Table 1), inhibited 5-[^{125}I]iodo-A-85380 binding and displayed pseudo-Hill coefficients (n_H) that did not differ significantly from 1. Recent data suggest that 5-[^{125}I]iodo-A-85380 has high affinity for nAChRs containing α6 subunits as well as for α4β2-nAChRs.[47] Nonetheless, in the rodent brain nAChRs containing the α6 subunit represent less than 10% of the available binding sites for this radioligand.[47,48] Consistent with this observation in the competition assay utilized in the present study, 1 μM α-conotoxin MII (a high affinity ligand for α6 containing nAChRs ($K_d \approx 1$ nM[56])) inhibited less than 5% of 5-[^{125}I]-iodo-A-85380 specific binding. Together, these results suggest that the affinities of the ligands measured in the present study reflect their affinities at α4β2-nAChRs.

Lipophilicity. The global log P, a common measure of lipophilicity, is a partition coefficient of non-ionized compounds between octanol and water. Chemical compounds containing groups that can form ions (for example, aliphatic amines such as A-85380 derivatives are protonated at pH 7.4) exist in water solution as a mixture of different ionic microspecies. The composition of this mixture depends on the ionization constant of the drug and the pH of the solution. In such cases, the partition coefficient log D_{pH} (apparent log P_{pH}) for dissociative systems gives a more appropriate description of complex partitioning equilibria:[49]

$$\log D = \log\left(\frac{\sum a_i^{org}}{\sum a_i^{H_2O}}\right) \quad (1)$$

where $a_i^{H_2O}$ is the concentration of ith microspecies in water and a_i^{org} is the concentration of ith microspecies in octanol. In this study, the *c*log $D_{7.4}$ values for all compounds in Table 1 were calculated using the ACD/LogD Suite software.[49]

Lipophilicity (log $D_{7.4}$) was also determined experimentally[50] for [^{18}F]**31**, [^{18}F]**35**, and 2-[^{18}F]fluoro-A-85380 (Table 1). Deviation of the calculated from the experimental results suggests that future QSAR studies with the members of this series should be done with experimentally acquired lipophilicity data.

Radiochemistry. A number of ligands in the series demonstrated high binding affinity for nAChRs along with a wide range of lipophilicities (see Table 1). These ligands are potential targets for radiolabeling and PET investigation in order to understand the role of lipophilicity in PET parameters (see Introduction). However, such an extensive investigation is beyond the scope of this report and will be the subject of future studies. Nevertheless, herein we report radiolabeling of two

Scheme 8[a]

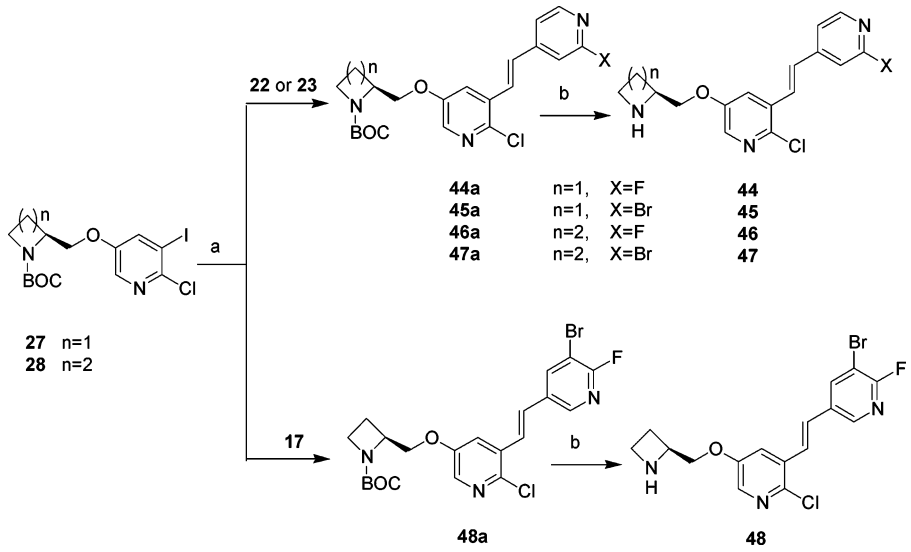

[a] Reagents: (a) 1,2,2,6,6-pentamethylpiperidine, Pd $(OAc)_2$, $(p\text{-tolyl})_3P$, acetonitrile; (b) TFA.

Scheme 9[a]

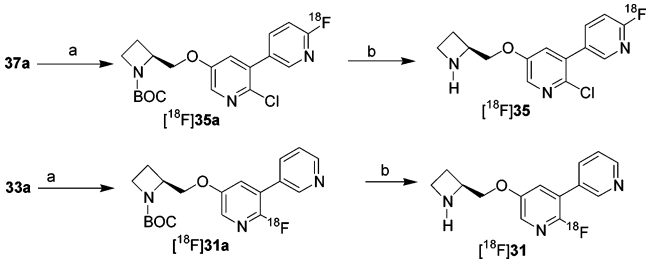

[a] Reagents: (a) [^{18}F]fluoride/Kryptofix222, DMSO, 185 °C; (b) TFA/CH_2Cl_2.

derivatives of the series, **31** and **35**, with [^{18}F] (Scheme 9) and the preliminary evaluation of these radioligands ([^{18}F]**31** and [^{18}F]**35)** in vivo. For both compounds, we targeted very high specific radioactivity to reduce in vivo occupancy of the cerebral nAChR (see Introduction).

The radiosynthesis of [^{18}F]**35** was performed by treatment of the corresponding BOC-protected bromo analogue **37a** with the K[^{18}F]F/Kryptofix222 complex[51] under the general conditions of Br−^{18}F exchange for 2-substituted pyridine derivatives developed elsewhere,[19] followed by deprotection of the intermediate [^{18}F]**35a** with trifluoroacetic acid. As expected, the incorporation of [^{18}F] required high temperature (185 °C), and the radiochemical yield of radiofluorination was 30−40% without optimization. To achieve high purity, both the intermediate [^{18}F]**35a** and the final [^{18}F]**35** were purified by semipreparative HPLC. After purification, the final [^{18}F]**35** was free of nonlabeled contaminants with a radiochemical yield of 5−10%, was radiochemically pure (>97% by radio HPLC), and coeluted with the standard **35**. The specific radioactivity of the final product prepared with 250−300 mCi [^{18}F]fluoride was in the range 7000−29000 mCi/μmol (end of synthesis, nondecay-corrected). The average time of the nonoptimized synthesis was 120 min.

Similarly, the radiosynthesis of [^{18}F]**31** was performed through the corresponding precursor **33a** with an overall radiochemical yield of 30% and a specific radioactivity in the range of 4000−8000 mCi/μmol (not presented in the Experimental Section).

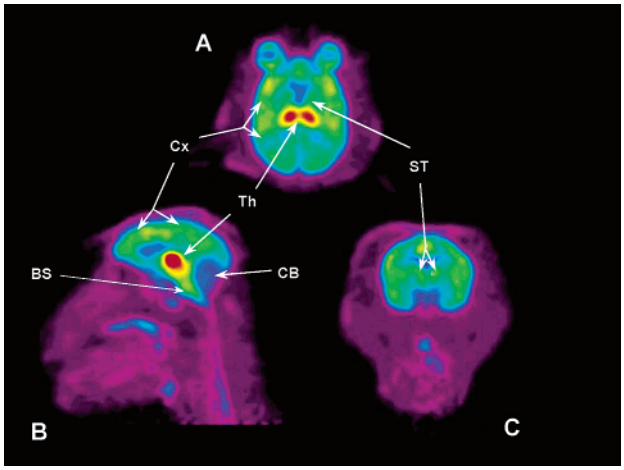

Figure 2. PET images of Rhesus monkey brain acquired from 390 to 450 min after [^{18}F]**35** injection: (A) transaxial view; (B) saggital view; (C) coronal view. The accumulation of radioactivity reflected the pattern of $\alpha4\beta2$-nAChRs distribution in the Rhesus monkey brain: thalamus (Th) > brain stem (BS), striatum (ST), cortical areas (CX) > cerebellum (CB). Accumulation of radioactivity is represented by pseudocolor coding (red > yellow > green > blue > purple).

The distribution pattern of compounds [^{18}F]**31** (data not presented) and [^{18}F]**35** in the Rhesus monkey brain (Figure 2) was consistent with the known distribution of the $\alpha4\beta2$-nAChRs[1] and similar to that of 2-[^{18}F]fluoro-A-85380.[34,52] BP* values in the thalamus and cortex for [^{18}F]**31** determined by the Logan method[53] were ca. 25−30% of those obtained with 2-[^{18}F]fluoro-A-85380. Since [^{18}F]**31** and 2-[^{18}F]fluoro-A-85380 exhibited similar binding affinity, the differences in the binding potential probably reflect their different lipophilicities (see Table 1).

At 7.5 h after injection of [^{18}F]**35**, the accumulated radioactivity in the focus regions of the Rhesus monkey brain, expressed as % ID, was 3- to 5-fold of those observed after administration of 2-[^{18}F]fluoro-A-85380.[34,52] In contrast, as shown in a separate PET study,[54] the BP* of [^{18}F]**35** in the thalamus, cortex, and striatum were ca. 2.5 times those of 2-[^{18}F]fluoro-A-85380[34] obtained in the same Rhesus monkeys. Therefore, these

results suggest that the novel radiotracer, [^{18}F]**35**, may be useful for quantitative imaging of extrathalamic nAChR and warrants an extensive PET investigation.

When other members of this series with various lipophilicities and low picomolar binding affinity are radiolabeled, the dependence of the imaging properties of these radioligands on their K_i and log D will be evaluated.

Structure−Activity Relationships. The primary goal of our study was to prepare compounds with binding affinities in the low picomolar range and with a wide range of lipophilicity. Targeted values of *c*log $D_{7.4}$ were ranged from −2 (as comparable with that for 2-fluoro-A-85380[38]) to +2 (to facilitate BBB permeability (see Introduction)). Because the development of PET imaging agents was our goal, the design of the target molecules required the presence of a fluoro or bromo substituent that would be suitable for radiolabeling with positron-emitting [^{18}F]fluorine or [^{76}Br]bromine.

We hypothesized that azetidinyl analogues of the lead compound **1**[36] (Table 1) should possess such properties. The replacement of pyrrolidinyl tail in **1** with azetidinyl should decrease the lipophilicity[49] and increase the ligand binding affinity, as this phenomenon was observed in another series.[38,41] Insertion of an appropriate substituent in the pyridine rings of **1** was another approach for improving of the binding affinity and controlling lipophilicity.

Consistent with our initial assumption, the novel azetidinyl analogue **32**, 5-pyridinyl derivative of A-98593 (Figure 1, Table 1), displayed high binding affinity at nAChRs. Replacement of the chlorine in molecule **32** with fluorine gave compound **31**, which exhibited lower binding affinity, whereas the affinities of the bromo- (**33**) or iodo- (**34**) analogues were more like that of **32**. The variation of K_i values within the subseries **31**−**34** prompted us to perform a molecular modeling study (see below).

To make a fluoro derivative of compound **32** with higher affinity, we chose (as suggested by molecular modeling below) to place the fluoro substituent in the terminal pyridine ring. The fluoro derivative **35** demonstrated the desirable high binding affinity. The replacement of fluorine in **35** with chlorine (**36**) or bromine (**37**) or addition of an additional bromine (**38**) yielded ligands with similar high affinity. A comparable trend was observed for the pyrrolidinyl analogues of this subseries, compounds **39** (F) and **40** (Br). Previously, we have shown that compound **2** exhibits a binding affinity for α4β2-nAChRs (K_i = 9 pM) at least as high as that of epibatidine.[38] Insertion of fluorine or bromine in the terminal pyridine ring of **2** gave compounds **44** and **45**, which also exhibit low picomolar affinity.

Molecular Modeling. As mentioned above, the fluoro analogue **31** exhibited approximately $^1/_{10}$ the binding affinity of the corresponding Cl-, Br-, and I-analogues (**32**, **33**, and **34**, respectively). Also, all analogues of compound **32** containing substituents in the external pyridine ring (**35**−**38**) displayed similar binding affinities. To investigate this phenomenon, we performed semiempirical quantum mechanical molecular calculations.

Sheridan's pharmacophore model[55] of nicotinic ligands is one of the currently accepted models that identify

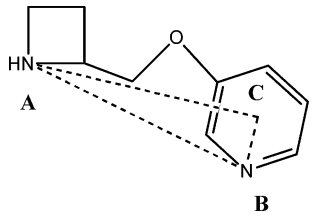

Figure 3. Sheridan's pharmacophoric elements A, B, and C of nAChR ligands as exemplified by A-85380.

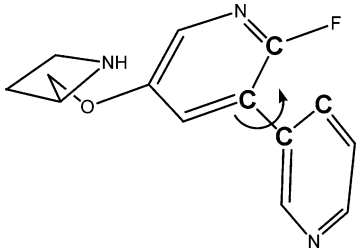

Figure 4. Conformer of compound **31** that was energy-optimized with respect to the dihedral angle. The carbon atoms forming the dihedral angle (see Table 2) are in bold.

important nicotinic receptor ligand geometries.[56] The model specifies three essential groups, such as a cationic center (A), an electronegative atom (B), and an atom (C), that form a dipole with B. In the case of nicotine, epibatidine, A-85380, and their analogues, the C atom is a pyridine ring centroid (Figure 3). These groups form a pharmacophore triangle with sides 4.8 Å (A−B), 4.0 Å (A−C), and 1.2 Å (B−C).[55] We have shown previously[57] that substitution on the pyridine ring of A-85380 analogues affects the geometry of the pharmacophoric triangle. Only the high-affinity members of the series displayed a tight fit superposition by the pharmacophoric triangle of the local low-energy conformers with (+)-epibatidine, a nicotinic agonist with very high binding affinity.[57]

Here, we have built the structures of **31**−**38** based on the low-energy conformer[57] of A-85380 using Chem3D software. The A-85380 conformer was then modified by addition of the necessary fragments provided by the software. To identify a low-energy conformation of these new structures, systematic searching of the dihedral angle around the bond connecting the two pyridine rings (Figure 4) was performed using an AM1 semiempirical protocol.

The calculated optimal values of the dihedral angle in these structures varied depending on the nature of the halogen attached to the internal pyridine ring, whereas the geometry of the Sheridan's pharmacophore for every compound of the series **31**−**38** did not vary (Table 2, Figure 5).

The binding affinity of the members of subseries **31**−**34** exhibited an excellent bell-shaped dependence on the value of the dihedral angle (Figure 6) around the bond connecting two pyridine rings. It is noteworthy that varying the halogen atoms attached to the external pyridine ring in equipotent ligands **35**−**38** exerted little effect on the values of their dihedral angle (Table 2, Figure 6).

Therefore, the binding affinity pattern within the subseries **31**−**38** cannot be explained only in terms of the Sheridan model. It is likely that the terminal heterocyclic ring connected at the C-5 position of the

Table 2. Calculated Dihedral Angle around the Bond Connecting Two Pyridine Rings and Pharmacophoric Distances for Compounds **31**−**38**

compd	dihedral angle, deg (see Figure 4)	A−B, Å	A−C, Å
A-85380[58]		4.39	4.43
31	−41	4.32	4.36
32	−57	4.33	4.39
33	−67	4.34	4.40
34	−85	4.35	4.41
36	−57	4.36	4.42
37	−57	4.32	4.37
35	−57	4.32	4.37
38	−58	4.31	4.35

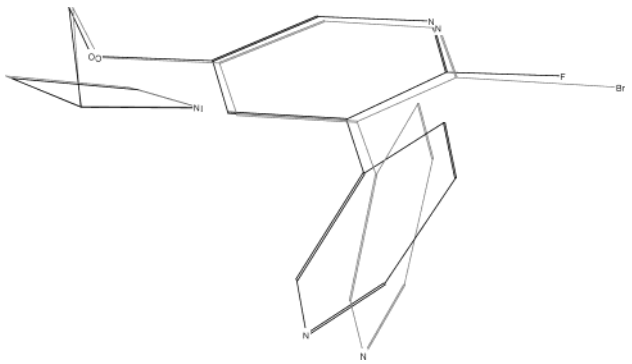

Figure 5. Superimposition of the low-energy conformers of **31** (solid black) and **33** (gray) by the three pharmacophoric elements.

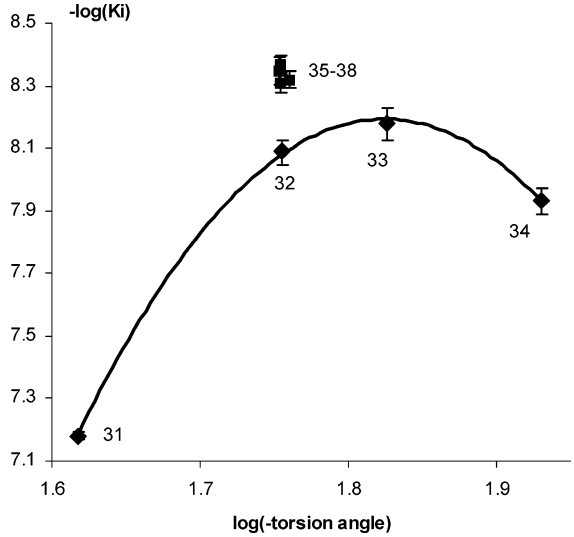

Figure 6. Relationship of binding affinity (−log(K_i), error bars = SEM) to the torsion angle around the bond connecting the pyridine rings (log(−torsion angle)) of compounds **31**−**34**. Derivatives of **32** having a halogen substituent in the external pyridine ring are compounds **35**−**38**.

internal pyridine ring is involved in the specific interaction with nAChR binding pocket perhaps through aromatic stacking with the benzene moiety of amino acids located within the nAChR binding domain.[58] This finding is in agreement with the idea that newer nicotinic agents may be using affinity-enhancing auxiliary binding sites not employed by nicotine and not accounted for by existing pharmacophore models.[59]

An important role of the C-5-substituents in the binding with nAChR is supported by the fact that A-85380 and epibatidine analogues containing hydrophobic and hydrogen-bonding substituents at the C-5 position of the pyridine ring exhibit improved binding affinity when compared with those of parent non-C-5-substituted analogues.[37,57,60]

Conclusion

A novel series of very high affinity ligands for α4β2-nAChRs has been developed. Lipophilicity within the series was broadly varied while maintaining low picomolar affinity. Fourteen ligands in the series exhibited higher binding affinities at α4β2-nAChRs than that of epibatidine.

Compounds with the highest binding affinity are analogues of A-98593 with halogenopyridinyl groups at position C-5 or derivatives of **2** that are halogenated at the terminal pyridine ring. Replacement of the Cl with F in the position C-6 of the internal pyridine ring of 5-pyridyl-A-98593 reduced the binding affinity.

Molecular modeling demonstrated that the binding affinities within the series **31**−**34** display a bell-shaped relationship with the value of the dihedral angle around the bond connecting two pyridine rings, suggesting an important role of orientation of the external heterocyclic rings on its interaction with nAChRs.

Two compounds, **31** and **35**, were radiolabeled with ^{18}F. Comparison of PET data for [^{18}F]**31** and 2-[^{18}F]FA, radioligands with similar binding affinity, showed the influence of lipophilicity on the binding potential. A preliminary study[54] with [^{18}F]**35** suggested that this radioligand holds promise for quantitative imaging extrathalamic nAChRs using PET.

Radiolabeling the presented series of nAChR ligands with positron-emitting isotopes will provide an opportunity to investigate the role of lipophilicity of nAChR radioligands on their imaging characteristics and, perhaps, to discover better imaging probes for PET research in humans.

Experimental Section

Chemistry. Unless specifically indicated, all reagents were purchased from Aldrich. All solvents used were ACS or HPLC grade. Microwave chemistry was done in a Discover oven (CEM Corporation, Mathews, NC). ^{1}H NMR spectra were recorded on a Bruker AM 300 (300 MHz) instrument; chemical shifts (δ) were recorded in parts per million (ppm) downfield from TMS. High-performance liquid chromatography (HPLC) analysis and purification were performed with a Rheodyne 7725 injector, a Waters 600 HPLC pump, and an in-line Waters 2487 dual λ absorbance detector (254 nm). HPLC chromatograms were recorded by a Rainin Dynamax dual channel control/interface module connected to a Macintosh computer with appropriate program software. Hamilton PRP-1 (10 μm, 7 mm × 305 mm), Waters Symmetry C-18 (3.5 μm, 4.6 mm × 150 mm), and Waters Nova-Pak C-18 radial compression (6 μm, 25 mm × 100 mm) columns were used in the HPLC analyses and preparative separations. Analytical thin-layer chromatography (TLC) was done on precoated plates of silica gel (0.25 mm, F254, Alltech). Flash chromatography was conducted using silica gel (230−400 mesh, Merck). Melting points were determined on a Mel-Temp II apparatus. Elemental analyses were performed at Galbraith Laboratories, Inc. and Quantitative Technologies, Inc (QTI). The newly synthesized final compounds gave satisfactory elemental analyses results (C, H, N, ±0.40%). The *c*log $D_{7.4}$ values were calculated using ACD/LogD Suite software.[49]

2-Bromo-3-iodo-5-nitropyridine (4). Phosphorus oxybromide (25.0 g, 87.2 mmol) was added to toluene (55 mL) at room temperature. Next, **3**[38] (21.1 g, 79.3 mmol) and quinoline (9.5 mL) were added consecutively to the mechanically stirred

reaction mixture at 90−100 °C. The vigorous reaction was monitored by TLC (ethyl acetate/hexane 5:15). After reaction completion, the toluene layer was separated. The remaining brownish solid was extracted with boiling toluene (3 × 260 mL). The combined toluene solutions were washed with 5% aqueous $NaHCO_3$, dried over anhydrous sodium sulfate, and concentrated by rotary evaporation. Flash column chromatography (95:5 hexane/ethyl acetate) workup gave **4** (21.1 g, 81.1%) as a yellow solid. Mp 107−109 °C. ^{1}H NMR ($CDCl_3$/TMS) δ: 9.15 (d, J = 2.5 Hz, 1H), 8.83 (d, J = 2.5 Hz, 1H).

5-Amino-2-bromo-3-iodopyridine (5). Compound **4** (18.6 g, 56.6 mmol) was added to a mixture of water (120 mL) and glacial acetic acid (180 mL). Iron powder (10.0 g) was then added to the reaction flask in small portions at 75 °C. After 15 min of mechanical stirring, the temperature rose to 85 °C. An additional 5.8 g of iron powder was added in two portions over a 2 h period with continuous stirring at 70−72 °C until TLC indicated a complete consumption of the precursor. Water (200 mL) was added to the reaction flask, and the mixture was made basic (pH 8) with sodium hydroxide solution. The mixture was then extracted with ethyl acetate (3 × 200 mL) and concentrated. Flash column chromatography (90:10 hexane/ethyl acetate) gave product **5** (12.5 g, 74%) as a white solid. Mp 128 °C. ^{1}H NMR ($CDCl_3$/TMS) δ: 7.83 (d, J = 2.7 Hz, 1H), 7.46 (d, J = 2.7 Hz, 1H), 3.72 (s, 2H).

5-Acetoxy-2-bromo-3-iodopyridine (6). Compound **5** (2.0 g, 6.7 mmol) was added to HBF_4 (25 mL, 50% solution) and cooled to 0 °C. A solution of sodium nitrite (0.6 g, 8.7 mmol) and water (10 mL) was added dropwise over a 35 min period. After the addition of sodium nitrite was complete, the mixture was stirred for 20 min at 0 °C. The reaction was monitored by TLC (ethyl acetate/hexane 5:15). The resulting diazonium salt was filtered, washed with cold diethyl ether (2 × 5 mL), and air-dried for 5 min. The solid was then dissolved in acetic anhydride (20 mL) and heated for 1 h at 70−85 °C. The solvent was evaporated, and the resulting residue was dissolved in diethyl ether (30 mL). The solvent was washed with water (4 × 15 mL), dried over magnesium sulfate, and evaporated under reduced pressure. Product **6** was obtained as an orange oil (2.17 g, 95%). ^{1}H NMR ($CDCl_3$/TMS) δ: 8.21 (d, J = 2.5 Hz, 1H), 7.94 (d, J = 2.5 Hz, 1H), 2.34 (s, 3H).

2-Bromo-5-hydroxy-3-iodopyridine (7). Compound **6** (2.17 g, 6.3 mmol) was added to a potassium hydroxide (15 mL, 2 N) and 2-propanol (20 mL) mixture at 0−5 °C. The precursor dissolved totally in 1 h to form a brownish, clear solution. The solution was acidified (pH 5) with acetic acid (∼1 mL) and extracted with ethyl acetate (3 × 30 mL). The combined extracts were washed with brine, dried over anhydrous sodium sulfate, and concentrated. The crude material (2.4 g) was redissolved in 20 mL of aqueous 2 N KOH. The solution was extracted with a mixture of hexane/ethyl acetate (1:1) to remove the remaining starting material. Next, the aqueous solution was acidified to pH 5 by acetic acid. Product **7**, a white solid, was precipitated from the solution, filtered, washed with water, and air-dried (1.44 g, 85%). Mp 189−191 °C. ^{1}H NMR (DMSO-d_6/TMS) δ: 7.95 (d, J = 2.8 Hz, 1H), 7.70 (d, J = 2.8 Hz, 1H).

2-Bromo-3-iodo-5-((1-(*tert*-butoxycarbonyl)-2-(*S*)-azetidinyl)methoxy)pyridine (8). Diethyl azodicarboxylate (DEAD, 69.7 mg, 0.4 mmol) and triphenylphosphine (104.9 mg, 0.4 mmol) were mixed in freshly distilled THF (1 mL) at 0 °C under an argon blanket until a solid paste was formed (15−20 min). *N*-BOC azetidinylmethanol (74.4 mg, 0.4 mmol) and **7** (100 mg, 0.3 mmol) were then added to the reaction flask, and the mixture was stirred at room temperature. The reaction was monitored by HPLC (80:20 acetonitrile/0.1 N ammonium formate, PRP-1 analytical column, 2 mL/min) and stopped after 19 h. The solvent was evaporated under reduced pressure at 55 °C, and the crude oil was purified via flash chromatography (90:10 hexane/ethyl acetate). Product **8** was obtained as a yellow oil (116 mg, 75%). ^{1}H NMR ($CDCl_3$/TMS) δ: 8.09 (d, J = 2.8 Hz, 1H), 7.72 (d, J = 2.8 Hz, 1H), 4.51 (m, 1H), 4.32 (m, 1H), 4.09 (m, 1H), 3.89 (m, 2H), 2.32 (m, 2H), 1.43 (s, 9H).

2-Amino-3-bromo-5-iodopyridine (13). *N*-Bromosuccinimide (NBS, 6.07 g, 34.1 mmol) was added slowly to a solution of 2-amino-5-iodopyridine (7.5 g, 34.1 mmol) in acetonitrile (150 mL). The reaction mixture was stirred at room temperature in darkness for 4 days. After reaction completion (TLC, hexane/ethyl acetate 1:1), the solution was filtered and concentrated under a vacuum. Gradient flash chromatography purification (80:20 hexane/ethyl acetate (800 mL), 70:30 hexane/ethyl acetate (600 mL)) produced **13** (5.9 g, 58%) as a yellow solid. Mp 106−110 °C. ^{1}H NMR ($CDCl_3$/TMS) δ: 8.16 (d, J = 1.9 Hz, 1H), 7.89 (d, J = 1.9 Hz, 1H), 4.93 (s, 2H).

3-Bromo-2-fluoro-5-iodopyridine (11). Sodium nitrite (0.67 g, 6.96 mmol) was added in small portions to a solution of **13** (1.8 g, 6.00 mmol) in an HF/pyridine mixture (25 mL) in a polyethylene reaction vessel cooled with an ice/salt bath. The resulting solution was stirred at 0 °C for 30 min, then heated to 40−50 °C and stirred at this temperature for 1 h. The reaction mixture was poured onto crushed ice (100 g), partially neutralized with sodium bicarbonate (pH 5), and extracted with ether (50 mL × 3). The combined extract was washed with water, dried over anhydrous sodium sulfate, and concentrated under the vacuum. Flash chromatography purification (70:30 hexane/ethyl acetate) produced **11** (1.69 g, 94%, mp 80−83 °C) as a white solid. ^{1}H NMR ($CDCl_3$/TMS) δ: 8.33 (m, 1H), 8.25 (dd, J = 2.0, 7.9 Hz, 1H).

2-Fluoro-5-iodopyrimidine (25). Sodium nitrite (0.72 g, 10.5 mmol) was added in small portions to a solution of 2-amino-5-iodopyrimidine (2.0 g, 9.05 mmol) in an HF/pyridine mixture (25 mL) in a polyethylene reaction vessel cooled with an ice/salt bath. The resulting solution was stirred at 0 °C for 30 min, then heated to 40−50 °C and stirred at this temperature for 1 h. The reaction mixture was poured onto crushed ice (100 g), partially neutralized with sodium bicarbonate (pH 5), and extracted with ether (70 mL × 3). The combined ether solution was washed with water, dried over anhydrous sodium sulfate and concentrated under the vacuum. Gradient flash column chromatography purification (80:20 hexane/ethyl acetate, 70:30 hexane/ethyl acetate) produced **25** (1.45 g, 72%, mp 121−124 °C) as a white solid. ^{1}H NMR ($CDCl_3$/TMS) δ: 8.81 (d, J = 1.6 Hz, 2H).

General Procedure for Preparing Trialkyltin Heteroarenes 14−16, 20, and 26. Iodoheteroarene (**9**, **10**, **11**, **18**, or **25**) (4.48 mmol), hexamethylditin (2.2 g, 6.73 mmol), and tetrakis(triphenylphosphine)palladium(0) (0.52 g, 0.45 mmol) were dissolved in anhydrous toluene (6.0 mL) in a sealed reaction vessel and stirred at 110−120 °C for 19−72 h. The reaction process was monitored by TLC (hexane/ethyl acetate). The resulting black reaction mixture was then filtered and concentrated at 50−60 °C. Gradient flash chromatography purification (95:5−80:20 hexane/ethyl acetate) produced the corresponding **14**, **15**, **16**, **20**, or **26** in 71−90% yield.

2-Fluoro-5-trimethyltinpyridine (14). The product was obtained as pale-yellow oil in 71% yield. ^{1}H NMR ($CDCl_3$/TMS) δ: 8.21 (m, 1H), 7.84 (m, 1H), 6.91 (dd, J = 2.2, 8.0 Hz, 1H), 0.34 (s, 9H).

2-Chloro-5-trimethyltinpyridine (15). The product was obtained as pale-yellow oil in 78.0% yield. ^{1}H NMR ($CDCl_3$/TMS) δ: 8.37 (dd, J = 0.9, 1.8 Hz, 1H), 7.71 (dd, J = 1.8, 7.7 Hz, 1H), 7.28 (dd, J = 0.9, 7.7 Hz, 1H), 0.35 (s, 1H).

2-Fluoro-3-bromo-5-Trimethyltinpyridine (16). The product was obtained as pale-yellow oil in 84.0% yield. ^{1}H NMR ($CDCl_3$/TMS) δ: 8.10 (s, 1H), 7.98 (dd, J = 1.5, 9.8 Hz, 1H), 0.37 (s, 1H).

2-Fluoro-4-trimethyltinpyridine (20). The product was obtained as colorless oil in 90% yield. ^{1}H NMR ($CDCl_3$/TMS) δ: 8.14 (d, J = 4.8 Hz, 1H), 7.25 (m, 1H), 7.05 (d, J = 3.4 Hz, 1H), 0.36 (s, 9H).

2-Fluoro-5-trimethyltinpyrimidine (26). The product was obtained as colorless oil in 90% yield. ^{1}H NMR ($CDCl_3$/TMS) δ: 8.61 (d, J = 2.6 Hz, 2H), 0.41 (s, 9H).

2-Bromo-4-trimethyltinpyridine (21). A 2.5 M solution of *n*-BuLi (0.34 mL, 0.84 mmol) was added drop by drop to a solution of freshly distilled tetramethylethylenediamine (TME-

DA, 0.12 mL, 0.77 mmol) in 5.3 mL of anhydrous ether cooled to −10 to −20 °C. The mixture was allowed to react at this temperature over 20 min and then cooled to −78 °C. A solution of 2-bromo-4-iodopyridine **19** (Specs and Biospecs Inc., Netherlands) (200 mg, 0.70 mmol) in anhydrous ether (1.8 mL) was added drop by drop at −78 °C. The resulting dark (apricot) mixture was allowed to react at this temperature over 30 min. Then a solution of trimethyltin chloride (168 mg, 0.84 mmol) in anhydrous ether (1.8 mL) was added over 7 min. The mixture was stirred at this temperature for 30 min and allowed to react overnight at room temperature. The reaction was then quenched with water, and the mixture was extracted with diethyl ether (25 mL × 3) and concentrated. Flash chromatography (80:20 hexane/ethyl acetate) gave product **21** (126 mg, 56%) as a pale-yellow oil. ^{1}H NMR ($CDCl_3$/TMS) δ: 8.26 (d, J = 4.6 Hz, 1H), 7.56 (s, 1H), 7.32 (d, J = 4.6 Hz, 1H), 0.36 (s, 9H).

General Procedure for Preparing Vinylpyridines 17, 22, and 23. Iodopyridine (**11**, **18**, or **19**; 3.16 mmol), tributyl(vinyl)tin (1.1 g, 3.48 mmol), and tetrakis(triphenylphosphine)-palladium(0) (0.47 g, 0.41 mmol) were dissolved in anhydrous toluene (7.0 mL). The reaction mixture was stirred at 110−125 °C for 18−24 h while it was monitored by HPLC (40:60 acetonitrile/water, Symmetry C18 column, 2 mL/min). After reaction completion, the mixture was concentrated at 50−60 °C. Gradient flash LC purification (hexane to 80:20 hexane/ethyl acetate) gave the corresponding products in 61−94% yield.

3-Bromo-2-fluoro-5-vinylpyridine (17). The product was obtained as pale-yellow oil in 94% yield. ^{1}H NMR ($CDCl_3$/TMS) δ: 8.11 (s, 1H), 8.03 (dd, J = 2.2, 8.2 Hz, 1H), 6.64 (dd, J = 11.0, 17.6 Hz, 1H), 5.78 (d, J = 17.6 Hz, 1H), 5.42 (d, J = 11.0 Hz, 1H).

2-Fluoro-4-vinylpyridine (22). The product was obtained as colorless oil in 94% yield. ^{1}H NMR ($CDCl_3$/TMS) δ: 8.16 (d, J = 5.2 Hz, 1H), 7.18 (m, 1H), 6.89 (s, 1H), 6.68 (dd, J = 10.8, 17.6 Hz, 1H), 5.99 (d, J = 17.6 Hz, 1H), 5.56 (d, J = 10.8 Hz, 1H).

2-Bromo-4-vinylpyridine (23). The product was obtained as pale-yellow oil in 75.2% yield. ^{1}H NMR ($CDCl_3$/TMS) δ: 8.31 (d, J = 5.2 Hz, 1H), 7.46 (d, J = 1.0 Hz, 1H), 7.23 (dd, J = 1.4, 5.2 Hz, 1H), 6.60 (dd, J = 10.8, 17.6 Hz, 1H), 5.98 (d, J = 17.6 Hz, 1H), 5.55 (d, J = 10.8 Hz, 1H).

General Procedure for Stille Coupling Reactions (Compounds 32a, 33a, and 35a−43a). An iodopyridyl ether (**8**, **27**, or **28**; 0.9 mmol), an appropriate trimethyltin heteroarene (**14**−**16**, **20**, **21**, **26**, **29**, or **30**; 1.2 mmol), and tetrakis-(triphenylphosphine)palladium(0) (54.8 mg, 0.05 mmol) were dissolved in anhydrous toluene (6.5 mL). The mixture was heated in a sealed reaction vessel and stirred at 110−130 °C for 30−103 h, except for compound **35a**, which was microwaved at 160 °C for an additional 2 h after 72 h of heating at 110 °C. The reaction process was monitored by HPLC (50:50 acetonitrile/water, 2−3 mL/min, Symmetry C18 column). The solvent was then evaporated at 50−60 °C. Final purification was done by gradient flash column chromatography (95:5 to 20:80 hexane/ethyl acetate). Compounds **32a** and **35a**−**43a** were obtained as pale-yellow oils, whereas **33a** was a pale-yellow solid.

6-Chloro-3-((1-(*tert*-butoxycarbonyl)-2-(*S*)-azetidinyl)-methoxy)-5-(pyridin-3-yl)pyridine (32a). The reagents are compounds **27** and **29**. The yield is 67.0%. ^{1}H NMR ($CDCl_3$/TMS) δ: 8.70 (d, J = 2.2 Hz, 1H), 8.67 (dd, J = 1.5, 4.9 Hz, 1H), 8.17 (d, J = 3.0 Hz, 1H), 7.83 (dt, J = 1.8, 7.9 Hz, 1H), 7.40 (dd, J = 4.9, 7.9 Hz, 1H), 7.29 (d, J = 3.0 Hz, 1H), 4.53 (m, 1H), 4.39 (m, 1H), 4.17 (dd, J = 3.0, 10.0 Hz, 1H), 3.89 (m, 2H), 2.34 (m, 2H), 1.40 (s, 9H).

6-Bromo-3-((1-(*tert*-butoxycarbonyl)-2-(*S*)-azetidinyl)-methoxy)-5-(pyridin-3-yl)pyridine (33a). The reagents are compounds **8** and **29**. The yield is 75.0%. ^{1}H NMR ($CDCl_3$/TMS) δ: 8.68 (m, 1H), 8.17 (d, J = 3.0 Hz, 1H), 7.80 (dt, J = 1.8, 7.9 Hz, 1H), 7.40 (dd, J = 4.9, 7.9 Hz, 1H), 7.25 (d, J = 3.0 Hz, 1H), 4.53 (m, 1H), 4.37 (m, 1H), 4.16 (dd, J = 2.8, 10.0 Hz), 3.89 (m, 2H), 2.34 (m, 2H), 1.40 (s, 9H).

6-Chloro-3-((1-(*tert*-butoxycarbonyl)-2-(*S*)-azetidinyl)-methoxy)-5-(6-fluoropyridin-3-yl)pyridine (35a). The reagents are compounds **27** and **14**. The yield is 76.0%. ^{1}H NMR ($CDCl_3$/TMS) δ: 8.30 (d, J = 2.7 Hz, 1H), 8.18 (d, J = 3.0 Hz, 1H), 7.94 (ddd, J = 2.7, 7.8, 8.4 Hz, 1H), 7.29 (d, J = 3.0 Hz, 1H), 7.05 (dd, J = 2.7, 8.4 Hz, 1H), 4.53 (m, 1H), 4.38 (m, 1H), 4.17 (dd, J = 3.0, 9.9 Hz), 3.89 (m, 2H), 2.33 (m, 2H), 1.40 (s, 9H).

6-Chloro-3-((1-(*tert*-butoxycarbonyl)-2-(*S*)-azetidinyl)-methoxy)-5-(6-chloropyridin-3-yl)pyridine (36a). The reagents are compounds **27** and **15**. The yield is 54.0%. ^{1}H NMR ($CDCl_3$/TMS) δ: 8.47 (d, J = 0.6, 2.5 Hz, 1H), 8.18 (d, J = 3.0 Hz, 1H), 7.80 (dd, J = 2.6, 8.3 Hz, 1H), 7.44 (dd, J = 0.5, 8.3 Hz, 1H), 7.28 (d, J = 3.0 Hz, 1H), 4.53 (m, 1H), 4.39 (m, 1H), 4.17 (dd, J = 2.8, 10.0 Hz, 1H), 3.89 (m, 2H), 2.34 (m, 2H), 1.40 (s, 9H).

6-Chloro-3-((1-(*tert*-butoxycarbonyl)-2-(*S*)-azetidinyl)-methoxy)-5-(6-bromopyridin-3-yl)pyridine (37a). The reagents are compounds **27** and **30**. The yield is 50.0%. ^{1}H NMR ($CDCl_3$/TMS) δ: 8.45 (dd, J = 0.7, 2.5 Hz, 1H), 8.18 (d, J = 3.0 Hz, 1H), 7.70 (dd, J = 2.5, 8.2 Hz, 1H), 7.60 (dd, J = 0.7, 8.2 Hz, 1H), 7.27 (d, J = 3.0 Hz, 1H), 4.53 (m, 1H), 4.39 (m, 1H), 4.17 (dd, J = 2.8, 10.1 Hz, 1H), 3.89 (m, 2H), 2.34 (m, 2H), 1.40 (s, 9H).

6-Chloro-3-((1-(*tert*-butoxycarbonyl)-2-(*S*)-azetidinyl)-methoxy)-5-(5-bromo-6-fluoropyridin-3-yl)pyridine (38a). The reagents are compounds **27** and **16**. The yield is 48.0%. ^{1}H NMR ($CDCl_3$/TMS) δ: 8.23 (dd, J = 1.1, 2.1 Hz, 1H), 8.19 (d, J = 3.0 Hz, 1H), 8.12 (dd, J = 2.2, 8.1 Hz, 1H), 7.28 (d, J = 3.0 Hz, 1H), 4.53 (m, 1H), 4.38 (m, 1H), 4.17 (dd, J = 2.8, 10.1 Hz), 3.89 (m, 2H), 2.33 (m, 2H), 1.40 (s, 9H).

6-Chloro-3-((1-(*tert*-butoxycarbonyl)-2-(*S*)-pyrrolidinyl)-methoxy)-5-(6-fluoropyridin-3-yl)pyridine (39a). The reagents are compounds **28** and **14**. The yield is 47.0%. ^{1}H NMR ($CDCl_3$/TMS) δ: 8.31 (m, 1H), 8.15 (d, J = 2.9 Hz, 1H), 7.94 (ddd, J = 2.6, 8.2, 8.4 Hz, 1H), 7.29 (m, 1H), 7.04 (dd, J = 2.8, 8.4 Hz, 1H), 4.22 (m, 1H), 4.14 (m, 1H), 4.01 (m, 1H), 3.37 (m, 2H), 2.03 (m, 2H), 1.91 (m, 2H), 1.45 (s, 9H).

6-Chloro-3-((1-(*tert*-butoxycarbonyl)-2-(*S*)-pyrrolidinyl)-methoxy)-5-(6-bromopyridin-3-yl)pyridine (40a). The reagents are compounds **28** and **30**.The yield is 62.0%. ^{1}H NMR ($CDCl_3$/TMS) δ: 8.46 (m, 1H), 8.16 (d, J = 3.0 Hz, 1H), 7.70 (dd, J = 2.5, 8.2 Hz, 1H), 7.59 (d, J = 8.2 Hz, 1H), 7.27 (m, 1H), 4.22 (m, 1H), 4.13 (m, 1H), 4.00 (m, 1H), 3.36 (m, 2H), 2.03 (m, 2H), 1.93 (m, 2H), 1.40 (s, 9H).

2-Chloro-5-((1-(*tert*-butoxycarbonyl)-2-(*S*)-azetidinyl)-methoxy)-3-(2-fluoropyridin-4-yl)pyridine (41a). The reagents are compounds **27** and **20**. The yield is 39.0%. ^{1}H NMR ($CDCl_3$/TMS) δ: 8.32 (d, J = 5.2 Hz, 1H), 8.21 (d, J = 3.0 Hz, 1H), 7.30 (m, 2H), 7.05 (brs, 1H), 4.53 (m, 1H), 4.40 (m, 1H), 4.17 (dd, J = 2.8, 10.1 Hz), 3.87 (m, 2H), 2.33 (m, 2H), 1.40 (s, 9H).

2-Chloro-5-((1-(*tert*-butoxycarbonyl)-2-(*S*)-azetidinyl)-methoxy)-3-(2-bromopyridin-4-yl)pyridine (42a). The reagents are compounds **27** and **21**. The yield is 44.0%. ^{1}H NMR ($CDCl_3$/TMS) δ: 8.48 (d, J = 5.1 Hz, 1H), 8.20 (d, J = 3.0 Hz, 1H), 7.60 (s, 1H), 7.39 (dd, J = 1.5, 5.1 Hz, 1H), 7.26 (s, 1H), 4.53 (m, 1H), 4.38 (m, 1H), 4.17 (dd, J = 2.8, 10.1 Hz), 3.89 (m, 2H), 2.33 (m, 2H), 1.40 (s, 9H).

2-Chloro-5-((1-(*tert*-butoxycarbonyl)-2-(*S*)-azetidinyl)-methoxy)-3-(6-fluoropyrimidin-3-yl)pyridine (43a). The reagents are compounds **27** and **26**. The yield is 50.0%. ^{1}H NMR ($CDCl_3$/TMS) δ: 8.78 (d, J = 1.6 Hz, 2H), 8.23 (d, J = 3.0 Hz, 1H), 7.33 (d, J = 2.8 Hz, 1H), 7.29 (d, J = 3.0 Hz, 1H), 7.05 (dd, J = 2.7, 8.4 Hz, 1H), 4.55 (m, 1H), 4.42 (m, 1H), 4.20 (dd, J = 2.8, 10.1 Hz), 3.89 (m, 2H), 2.33 (m, 2H), 1.40 (s, 9H).

6-Fluoro-3-((1-(*tert*-butoxycarbonyl)-2-(*S*)-azetidinyl)-methoxy)-5-(pyridin-3-yl)pyridine (31a). Compound **33a** (84 mg, 0.2 mmol) and tetrabutylammonium fluoride (1.0 M THF solution, 2 mL, 2.0 mmol) were dissolved in anhydrous DMSO (1.5 mL). The mixture was stirred at 150 °C for 18 h, and the reaction was monitored by HPLC (60:40 acetonitrile/0.4% acetic acid water solution, PRP-1 (250 mm × 4.1 mm), 3 mL/min). Next, the mixture was mixed with 0.5% acetic acid

aqueous solution (45 mL), extracted with methylene chloride (20 mL × 5), and concentrated under the vacuum. The product was purified via the preparative HPLC (40:60 acetonitrile/water, Novapak C18, 20 mm × 100 mm column, 12 mL/min). The collected product fraction was concentrated by rotary evaporation. The aqueous phase was saturated with sodium sulfate and extracted with methylene chloride. The solvent was removed to reveal product **31a** as a yellow oil (29 mg, 40%). ^{1}H NMR ($CDCl_3$/TMS) δ: 8.82 (m, 1H), 8.67 (m, 1H), 7.92 (m, 2H), 7.50 (dd, J = 2.9, 7.9 Hz, 1H), 7.42 (m, 1H), 4.54 (m, 1H), 4.39 (m, 1H), 4.18 (dd, J = 2.8, 10.0 Hz), 3.90 (m, 2H), 2.35 (m, 2H), 1.41 (s, 9H).

6-Iodo-3-((1-(*tert*-butoxycarbonyl)-2-(*S*)-azetidinyl)-methoxy)-5-(pyridin-3-yl)pyridine (34a). Compound **33a** (62.7 mg, 0.15 mmol), copper(I) iodide (1.4 g, 7.5 mmol), and potassium iodide (1.2 g, 7.5 mmol) were dissolved in anhydrous DMSO (1.0 mL). The mixture was stirred at 140 °C for 110 min while the reaction was monitored by HPLC (50:50 acetonitrile/1.0 N ammonium formate water solution, symmetry C-18 analytical column (4.6 mm × 150 mm), 2 mL/min). Then the mixture was poured into water (20 mL), filtered through Celite, and extracted with ethyl acetate (3 × 20 mL). Concentration under the vacuum produced 55 mg of crude **34a** as a yellow oil. The crude product was further purified via preparative HPLC (45:55 acetonitrile/water, Nova-Pak C-18, 20 mm × 100 mm column, 12 mL/min). The collected product fraction was concentrated by rotary evaporation. The aqueous phase was basified by sodium bicarbonate powder (pH 9) and extracted with methylene chloride. The organic solvent was dried and removed, yielding product **34a** as a pale-yellow oil (46 mg, 67%). ^{1}H NMR ($CDCl_3$/TMS) δ: 8.69 (m, 1H), 8.63 (m, 1H), 8.19 (d, J = 3.0 Hz, 1H), 7.73 (dt, J = 1.8, 6.1 Hz, 1H), 7.40 (dd, J = 4.9, 7.9 Hz, 1H), 7.16 (d, J = 3.0 Hz, 1H), 4.52 (m, 1H), 4.36 (m, 1H), 4.15 (dd, J = 2.9, 10.0 Hz), 3.89 (m, 2H), 2.33 (m, 2H), 1.39 (s, 9H).

General Procedure for Heck Coupling Reactions (Compounds 44a−48a). Iodopyridyl ether **27** or **28** (1.10 mmol) and vinylpyridine derivative **22**, **23**, or **17** (1.10 mmol) were dissolved in anhydrous acetonitrile (5 mL). 1,2,2,6,6-Pentamethylpiperidine (343 mg, 2.21 mmol), palladium(II) acetate (50 mg, 0.22 mmol), and tri-*o*-tolylphosphine (15 mg, 0.22 mmol) were then added to the solution. The mixture was stirred at 100 °C for 12−82 h while the reaction completion was monitored by HPLC (50:50 or 60:40 acetonitrile/water, symmetry column, 4.6 mm × 150 mm). The reaction mixture was filtered and concentrated under the vacuum. Gradient flash LC purification (90:10 to 50:50 hexane/ethyl acetate) produced compounds **44a**−**48a** as yellow oils.

2-Chloro-5-((1-(*tert*-butoxycarbonyl)-2-(*S*)-azetidinyl)-methoxy)-3-(2-(2-fluoropyridin-4-yl)vinyl)pyridine (44a). The yield is 60%. ^{1}H NMR ($CDCl_3$/TMS) δ: 8.24 (d, J = 5.2 Hz, 1H), 8.10 (d, J = 2.9 Hz, 1H), 7.62 (m, 1H), 7.57 (d, J = 16.3 Hz, 1H), 7.33 (dt, J = 1.5, 3.7 Hz, 1H), 7.07 (d, J = 16.3 Hz, 1H), 7.03 (s, 1H), 4.54 (m, 1H), 4.43 (m, 1H), 4.21 (dd, J = 2.6, 10.2 Hz, 1H), 3.90 (m, 2H), 2.35 (m, 2H), 1.42 (s, 9H).

2-Chloro-5-((1-(*tert*-butoxycarbonyl)-2-(*S*)-azetidinyl)-methoxy)-3-(2-(2-bromopyridin-4-yl)vinyl)pyridine (45a). The yield is 72%. ^{1}H NMR ($CDCl_3$/TMS) δ: 8.38 (d, J = 5.2 Hz, 1H), 8.10 (d, J = 2.9 Hz, 1H), 7.61 (m, 2H), 7.55 (d, J = 16.4 Hz, 1H), 7.38 (dd, J = 1.4, 5.2 Hz, 1H), 7.01 (d, J = 16.6 Hz), 4.54 (m, 1H), 4.43 (m, 1H), 4.21 (dd, J = 2.4, 10.6 Hz, 1H), 3.90 (m, 2H), 2.36 (m, 2H), 1.42 (s, 9H).

2-Chloro-5-((1-(*tert*-butoxycarbonyl)-2-(*S*)-pyrrolidinyl)-methoxy)-3-(2-(2-fluoropyridin-4-yl)vinyl)pyridine (46a). The yield is 32%. ^{1}H NMR ($CDCl_3$/TMS) δ: 8.23 (d, J = 5.1 Hz, 1H), 8.06 (d, J = 2.9 Hz, 1H), 8.03 (m, 1H), 7.58 (d, J = 16.4 Hz, 1H), 7.34 (m, 1H), 7.31 (d, J = 16.4 Hz, 1H), 7.04 (brs, 1H), 4.32 (m, 1H), 4.15 (m, 1H), 3.96 (m, 1H), 3.41 (m, 1H), 3.33 (m, 1H), 2.01 (m, 2H), 1.92 (m, 2H), 1.50 (s, 9H).

2-Chloro-5-((1-(*tert*-butoxycarbonyl)-2-(*S*)-pyrrolidinyl)-methoxy)-3-(2-(2-bromopyridin-4-yl)vinyl)pyridine (47a). The yield is 55%. ^{1}H NMR ($CDCl_3$/TMS) δ: 8.37 (d, J = 5.1 Hz, 1H), 8.08 (m, 1H), 8.06(d, J = 2.9 Hz, 1H), 7.62 (s, 1H), 7.56 (J = 16.4 Hz, 1H), 7.42 (d, J = 4.7 Hz, 1H), 7.28 (d, J = 16.4 Hz, 1H), 4.32 (m, 1H), 4.13 (m, 1H), 3.94 (dd, J = 8.4, 9.8 Hz, 1H), 3.41 (m, 1H), 3.32 (m, 1H), 2.01 (m, 2H), 1.93 (m, 2H), 1.51 (s, 9H).

2-Chloro-5-((1-(*tert*-butoxycarbonyl)-2-(*S*)-azetidinyl)-methoxy)-3-(2-(6-fluoro-5-bromopyridin-3-yl)vinyl)pyridine (48a). The yield is 60%. ^{1}H NMR ($CDCl_3$/TMS) δ: 8.25 (brs, 1H), 8.20 (dd, J = 2.2, 8.1 Hz, 1H), 8.08 (d, J = 2.9 Hz, 1H), 7.61 (m, 1H), 7.34 (d, J = 16.4 Hz, 1H), 7.05 (d, J = 16.4 Hz, 1H), 4.54 (m, 1H), 4.43 (m, 1H), 4.20 (dd, J = 2.2, 10.1 Hz, 1H), 3.90 (m, 2H), 2.35 (m, 2H), 1.42 (s, 9H).

6-Fluoro-3-((2-(*S*)-azetidinyl)methoxy)-5-(pyridin-3-yl)pyridine (31) and General Procedure for Compounds 32−48. Trifluoroacetic acid (TFA, 0.5 mL, 6.5 mmol) was added to a solution of **31a** (61 mg, 0.17 mmol) in dichloromethane (2 mL). The mixture was stirred overnight at room temperature and the solvent was removed by rotary evaporation at 50−60 °C to reveal **31**·TFA (120 mg, 100% yield) as a viscous yellow oil. ^{1}H NMR (acetone-d_6) δ: 8.91 (brs, 1H), 8.74 (brs, 1H), 8.42 (ddd, J = 1.6, 3.1, 8.1 Hz, 1H), 7.88 (m, 3H), 5.55 (m, 1H), 4.84 (m, 1H), 4.67 (m, 3H), 2.79 (m, 1H), 2.41 (m, 1H). Anal. Calcd for $C_{14}H_{14}FN_3O$·4.1TFA.

6-Chloro-3-((2-(*S*)-azetidinyl)methoxy)-5-(pyridin-3-yl)pyridine (32), salt with TFA. 100% yield. ^{1}H NMR ($CDCl_3$/TMS) δ: 8.89 (brs, 1H), 8.76 (brs, 1H), 8.31 (d, J = 8.0 Hz, 1H), 8.18 (s, 1H), 7.78 (m, 1H), 7.46 (brs, 1H), 4.87 (m, 1H), 4.41 (m, 2H), 4.08 (m, 2H), 2.70 (m, 2H). Anal. Calcd for $C_{14}H_{14}ClN_3O$·2.82TFA.

6-Bromo-3-((2-(*S*)-azetidinyl)methoxy)-5-(pyridin-3-yl)pyridine (33), salt with TFA. 100% yield. ^{1}H NMR ($CDCl_3$/TMS) δ: 8.92 (brs, 1H), 8.80 (brs, 1H), 8.44 (d, J = 8.2 Hz, 1H), 8.20 (s, 1H), 7.90 (m, 1H), 7.42 (brs, 1H), 4.86 (m, 1H), 4.42 (m, 2H), 4.10 (m, 2H), 2.71 (m, 2H). Anal. Calcd for $C_{14}H_{14}BrN_3O$·2.91 TFA·0.25H_2O.

6-Iodo-3-((2-(*S*)-azetidinyl)methoxy)-5-(pyridin-3-yl)-pyridine (34), salt with TFA. 100% yield. ^{1}H NMR ($CDCl_3$/TMS) δ: 8.90 (brs, 1H), 8.84 (d, J = 5.0 Hz, 1H), 8.44 (d, J = 7.6 Hz, 1H), 8.25 (d, J = 2.8 Hz, 1H), 7.94 (dd, J = 5.6, 7.7 Hz, 1H), 7.34 (d, J = 2.8 Hz, 1H), 4.93 (m, 1H), 4.41 (m, 2H), 4.10 (m, 2H), 2.74 (m, 2H). Anal. Calcd for $C_{14}H_{14}IN_3O$·3.38 TFA·0.26H_2O.

6-Chloro-3-((2-(*S*)-azetidinyl)methoxy)-5-(6-fluoropyridin-3-yl)pyridine (35), salt with TFA. 100% yield. ^{1}H NMR ($CDCl_3$/TMS) δ: 8.29 (d, J = 2.7 Hz, 1H), 8.21 (d, J = 3.0 Hz, 1H), 7.97 (ddd, J = 2.7, 7.8, 8.4 Hz, 1H), 7.37 (d, J = 3.0 Hz, 1H), 7.10 (dd, J = 2.7, 8.4 Hz, 1H), 4.97 (m, 1H), 4.40 (m, 2H), 4.16 (m, 2H), 2.78 (m, 2H). Anal. Calcd for $C_{14}H_{13}N_3ClFO$·3.38TFA.

6-Chloro-3-((2-(*S*)-azetidinyl)methoxy)-5-(6-chloropyridin-3-yl)pyridine (36), salt with TFA. 100% yield. ^{1}H NMR ($CDCl_3$/TMS) δ: 8.47 (d, J = 2.4 Hz, 1H), 8.20 (d, J = 3.0 Hz, 1H), 7.85 (dd, J = 2.5, 8.3 Hz, 1H), 7.49 (d, J = 8.3 Hz, 1H), 7.35 (d, J = 3.0 Hz, 1H), 4.94 (m, 1H), 4.40 (m, 2H), 4.14 (m, 2H), 2.76 (m, 2H). Anal. Calcd for $C_{14}H_{13}N_3Cl_2O$·2.7TFA.

6-Chloro-3-((2-(*S*)-azetidinyl)methoxy)-5-(6-bromopyridin-3-yl)pyridine (37), salt with TFA. 100% yield. ^{1}H NMR ($CDCl_3$/TMS) δ: 8.46 (d, J = 2.4 Hz, 1H), 8.19 (d, J = 3.0 Hz, 1H), 7.74 (dd, J = 2.4, 8.2 Hz, 1H), 7.64 (d, J = 8.2 Hz, 1H), 7.36 (d, J = 3.0 Hz), 4.94 (m, 1H), 4.40(m, 2H), 4.14 (m, 2H), 2.74 (m, 2H). Anal. Calcd for $C_{14}H_{13}N_3BrClO$·2.68 TFA·0.6H_2O.

6-Chloro-3-((2-(*S*)-azetidinyl)methoxy)-5-(5-bromo-6-fluoropyridin-3-yl)pyridine (38), salt with TFA. 100% yield. ^{1}H NMR ($CDCl_3$/TMS) δ: 8.21 (m, 2H), 8.11 (d, J = 8.1 Hz, 1H), 7.33 (m, 1H), 4.98 (m, 1H), 4.40 (m, 2H), 4.16 (m, 2H), 2.79 (m, 2H). Anal. Calcd for $C_{14}H_{12}N_3BrClFO$·2.81TFA.

6-Chloro-3-((2-(*S*)-pyrrolidinyl)methoxy)-5-(6-fluoropyridin-3-yl)pyridine (39), salt with TFA. 100% yield. ^{1}H NMR ($CDCl_3$/TMS) δ: 8.28 (d, J = 2.5 Hz, 1H), 8.15 (d, J = 2.9 Hz, 1H), 7.94 (ddd, J = 2.5, 7.5, 8.4 Hz, 1H), 7.30 (d, J = 3.0 Hz, 1H), 7.07 (dd, J = 2.7, 8.5 Hz, 1H), 4.34 (m, 2H), 4.10 (m, 1H), 3.42 (m, 2H), 2.16 (m, 4H). Anal. Calcd for $C_{15}H_{15}N_3ClFO$·2.02TFA·0.9H_2O.

6-Chloro-3-((2-(*S*)-pyrrolidinyl)methoxy)-5-(6-bromopyridin-3-yl)pyridine (40), salt with TFA. 100% yield. ^{1}H

NMR ($CDCl_3$/TMS) δ: 8.45 (d, J = 2.2 Hz, 1H), 8.15 (d, J = 2.9 Hz, 1H), 7.73 (dd, J = 2.5, 8.3 Hz, 1H), 7.63 (d, J = 8.3 Hz, 1H), 7.30 (d, J = 3.0 Hz, 1H), 4.40 (dd, J = 3.5, 10.3 Hz, 1H), 4.29 (m, 1H), 4.10 (m, 1H), 3.42 (m, 2H), 2.16 (m, 4H). Anal. Calcd for $C_{15}H_{15}N_3ClBrO\cdot 2.89TFA$.

2-Chloro-5-((2-(*S*)-azetidinyl)methoxy)-3-(2-fluoropyridin-4-yl)pyridine (41), salt with TFA. 100% yield. ^{1}H NMR ($CDCl_3$/TMS) δ: 8.35 (d, J = 5.2 Hz, 1H), 8.22 (d, J = 2.9 Hz, 1H), 7.36 (d, J = 3.0 Hz, 1H), 7.31 (dt, J = 1.5, 5.1 Hz, 1H), 7.06 (brs, 1H), 4.92 (m, 1H), 4.41 (d, J = 3.8 Hz, 2H), 4.13 (m, 2H), 2.74 (m, 2H). Anal. Calcd for $C_{14}H_{13}N_3ClFO\cdot 2.16TFA\cdot 0.48H_2O$.

2-Chloro-5-((2-(*S*)-azetidinyl)methoxy)-3-(2-bromopyridin-4-yl)pyridine (42), salt with TFA. 100% yield. ^{1}H NMR ($CDCl_3$/TMS) δ: 8.55 (d, J = 5.2 Hz, 1H), 8.24 (d, J = 2.9 Hz, 1H), 7.62 (s, 1H), 7.43 (dd, J = 1.4, 5.1 Hz, 1H), 7.35 (d, J = 2.9 Hz, 1H), 4.96 (m, 1H), 4.39 (m, 2H), 4.15 (m, 2H), 2.78 (m, 2H). Anal. Calcd for $C_{14}H_{13}N_3ClBrO\cdot 2.99TFA$.

2-Chloro-5-((2-(*S*)-azetidinyl)methoxy)-3-(6-fluoropyrimidin-3-yl)pyridine (43), salt with TFA. 100% yield. ^{1}H NMR ($CDCl_3$/TMS) δ: 8.77 (d, J = 1.5 Hz, 2H), 8.30 (d, J = 2.9 Hz, 1H), 7.39 (d, J = 3.0 Hz, 1H), 4.95 (m, 1H), 4.40 (m, 2H), 4.17 (m, 2H), 2.74 (m, 2H). Anal. Calcd for $C_{13}H_{12}N_4ClFO\cdot 2.81TFA\cdot 0.42H_2O$.

2-Chloro-5-((2-(*S*)-azetidinyl)methoxy)-3-(2-(2-fluoropyridin-4-yl)vinyl)pyridine (44), salt with TFA. 100% yield. ^{1}H NMR ($CDCl_3$/TMS) δ: 8.28 (d, J = 5.4 Hz, 1H), 8.14 (d, J = 2.9 Hz, 1H), 7.69 (d, J = 2.9 Hz, 1H), 7.55 (d, J = 16.4 Hz, 1H), 7.36 (d, J = 5.3 Hz, 1H), 7.07 (d, J = 16.4 Hz, 1H), 7.06 (s, 1H), 4.98 (m, 1H), 4.42 (m, 2H), 4.20 (m, 2H), 2.80 (m, 2H). Anal. Calcd for $C_{16}H_{15}N_3ClFO\cdot 3.15TFA\cdot 0.9H_2O$.

2-Chloro-5-((2-(*S*)-azetidinyl)methoxy)-3-(2-(2-bromopyridin-4-yl)vinyl)pyridine (45), salt with TFA. 100% yield. ^{1}H NMR ($CDCl_3$/TMS) δ: 8.48 (d, J = 5.3 Hz, 1H), 8.15 (d, J = 2.9 Hz, 1H), 7.68 (d, J = 3.0 Hz, 1H), 7.66 (s, 1H), 7.56 (d, J = 16.4 Hz, 1H), 7.46 (dd, J = 1.4, 5.4 Hz, 1H), 7.02 (d, J = 16.4 Hz, 1H), 5.08 (m, 1H), 4.42 (m, 2H), 4.20 (m, 2H), 2.80 (m, 2H). Anal. Calcd for $C_{16}H_{15}N_3ClBrO\cdot 3.51TFA$.

2-Chloro-5-((2-(*S*)-pyrrolidinyl)methoxy)-3-(2-(2-fluoropyridin-4-yl)vinyl)pyridine (46), salt with TFA. 100% yield. ^{1}H NMR ($CDCl_3$/TMS) δ: 8.27 (d, J = 5.4 Hz, 1H), 8.08 (d, J = 2.8 Hz, 1H), 7.62 (d, J = 2.8 Hz, 1H), 7.52 (d, J = 16.4 Hz, 1H), 7.35 (m, 1H), 7.06 (d, J = 16.4 Hz, 1H), 7.06 (s, 1H), 4.41 (dd, J = 3.6, 10.2 Hz, 1H), 4.31 (m, 1H), 4.12 (m, 1H), 3.46 (m, 2H), 2.19 (m, 4H). Anal. Calcd for $C_{17}H_{17}N_3ClFO\cdot 2.8TFA\cdot 0.5H_2O$.

2-Chloro-5-((2-(*S*)-pyrrolidinyl)methoxy)-3-(2-(2-bromopyridin-4-yl)vinyl)pyridine (47), salt with TFA. 100% yield. ^{1}H NMR ($CDCl_3$/TMS) δ: 8.46 (d, J = 5.3 Hz, 1H), 8.08 (d, J = 2.6 Hz, 1H), 7.65 (s, 1H), 7.60 (d, J = 2.7 Hz, 1H), 7.53 (d, J = 16.4 Hz, 1H), 7.44 (dd, J = 1.3, 5.3 Hz, 1H), 7.00 (d, J = 16.4 Hz, 1H), 4.34 (m, 2H), 4.11 (m, 1H), 3.46 (m, 2H), 2.16 (m, 4H). Anal. Calcd for $C_{17}H_{17}N_3ClBrO\cdot 3.8TFA\cdot 0.14H_2O$.

2-Chloro-5-((2-(*S*)-azetidinyl)methoxy)-3-(2-(6-fluoro-5-bromopyridin-3-yl)vinyl)pyridine (48), salt with TFA. 100% yield. ^{1}H NMR ($CDCl_3$/TMS) δ: 8.23 (s, 1H), 8.22 (dd, J = 1.8, 8.1 Hz, 1H), 8.10 (d, J = 2.0 Hz, 1H), 7.65 (d, J = 2.0 Hz, 1H), 7.32 (d, J = 16.5 Hz, 1H), 7.04 (d, J = 16.5 Hz, 1H), 4.96 (m, 1H), 4.40 (m, 2H), 4.17 (m, 2H), 2.78 (m, 2H). Anal. Calcd for $C_{16}H_{14}N_3FClBrO\cdot 3.1TFA$.

Radiochemistry. 6-Chloro-3-((2-(*S*)-azetidinyl)methoxy)-5-(2-[^{18}F]fluoropyridin-5-yl)pyridine, [^{18}F]35a. An aqueous solution of the [^{18}F]fluoride, 25 mg of Kryptofix 222, and 4.5 mg of K_2CO_3 was added to a 10 mL vessel. The mixture was heated in an oil bath at 120−135 °C under a stream of argon while water was evaporated azeotropically using repeated additions of anhydrous CH_3CN. A solution of the bromo precursor **37a** (3 mg) in anhydrous DMSO (0.7 mL) was added to the reaction vessel and heated at 185 °C for 20 min. The reaction mixture was cooled, diluted with 1 mL of water, injected onto the reverse-phase HPLC column (Hamilton PRP-1, 7 mm × 300 mm), and eluted with a mixture of acetonitrile/water (53:47) at a flow rate of 6 mL/min. The radioactive peak of [^{18}F]**35a** with a retention time of 15−16 min was collected into a flask with 1 mL of trifluoroacetic acid, and the solvent was removed on a rotary evaporator (65 °C). The residue was dissolved in 3 mL of trifluoroacetic acid and heated at 65 °C for 15 min. The solvent was evaporated again on a rotary evaporator, and the residue was redissolved in the mobile phase (CH_3CN/0.2% aqueous CF_3COOH, 17:83), injected onto the HPLC column, and eluted at a flow rate of 6 mL/min. The radioactive peak of [^{18}F]**35** with a retention time of 13 min was collected, and the solvent was removed on a rotary-evaporator. The product [^{18}F]**35** was dissolved in saline (5 mL) and filtered through a sterile filter unit.

An aliquot of the final solution of known volume and radioactivity was applied to an analytical HPLC column (Hamilton, PRP-1, 2.1 mm × 250 mm). A mobile phase of CH_3CN/0.2% aqueous CF_3COOH, 23:77, at a flow rate of 2 mL/min was used to elute the radioligand, which had a retention time of 4.4−4.7 min. The radiochemical purity was greater than 99%. The area of the UV absorbance peak at 254 nm corresponding to the carrier product **35** was measured and compared to the standard calibration curve relating mass to UV absorbance. In 11 production runs, the specific radioactivity ranged from 7000 to 29000 mCi/μmol. The radiochemical product also coeluted with a sample of **35**.

Molecular Modeling. The systematic searching of the dihedral angle around the bond connecting the pyridine rings in 30° increments followed by full optimization of the conformer with the lowest formation energy was performed using the AM1 protocol available through CS Chem3D Pro software (CambridgeSoft Corporation, Cambridge, MA).

In Vitro Binding Assay. Competition assays with 5-[^{125}I]-iodo-A-85380 (5-[^{125}I]IA) were performed as described previously.[46] Crude membrane fractions (P2) were prepared from frozen Sprague-Dawley rat brains (excluding medulla and cerebellum) obtained from Pel-Freez Biologicals (Rogers, AR). P2 membranes (5−7 μg of protein) were incubated in a total volume of 0.4 mL of HEPES salt solution (pH 7.4) with 50 pM 5-[^{125}I]IA and one of nine concentrations of the test compounds. Samples were incubated for 3 h at 23 °C. All assays were performed in polystyrene titer plates (Beckman Instruments Co., Columbia, MD). Nonspecific binding was determined in the presence of 300 μM (−)-nicotine. The binding was terminated by a vacuum filtration through GF/B filters pretreated with 1% polyethyleneimine. Experiments were performed in duplicate. The K_i values were calculated with the Cheng−Prusoff equation, $K_i = IC_{50}/(1 + F/K_D)$, where F is the concentration of unbound radioligand. The K_D value for 5-[^{125}I]-IA of 10 pM (at 23 °C) measured in direct binding assays was used for the calculations. Direct binding assays were performed on aliquots of the same membrane preparations that were used for the competition assays. The competition binding data were analyzed using nonlinear regression analysis and the "Solver program" incorporated in Microsoft Excel for Windows, version 9.0.

PET Studies. All experiments involving research animals were approved by the Animal Care and Use Committee (ACUC) of the NIDA Intramural Research Program.

The PET scans of two Rhesus monkeys, 13 and 8 kg body weight and ca. 8 years old, were performed under Saffan anesthesia after intravenous bolus injection of 1.2 mCi/kg of [^{18}F]**31** (specific activity at injection time was 5300 Ci/mmol) and 1.7 mCi/kg of [^{18}F]**35** (specific activity at injection time was 10800 Ci/mmol). In the present study the cerebellum (Cb) was used as a reference region for the calculation of nondisplaceable volume of distribution (VDnds) and BP* of [^{18}F]**31** in the thalamus. A previous study[34] demonstrated that Cb contains very low density of $\alpha 4\beta 2$-nAChRs compared to the density in the thalamus and can be used as a measure of VDnds for the Rhesus monkey thalamus. Thirty dynamic PET scans with gradually increasing duration (from 3 to 20 min) were acquired over 8 h on a Siemens Exact ECAT HR+ whole-body tomograph in 3D mode (PET procedures and image reconstruction were described in detail elsewhere[34,52]).

Acknowledgment. The authors thank Drs. Elliot Stein, D. Bruce Vaupel, Amy H. Newman, and Santosh

Kulkarni for their helpful discussions, and Ms. Mary Pfeiffer for her kind editorial assistance.

References

(1) Decker, M. W.; Brioni, J. D.; Bannon, A. W.; Arneric, S. P. Diversity of neuronal nicotinic acetylcholine receptors: lessons from behavior and implications for CNS therapeutics. *Life Sci.* **1995**, *56*, 545−570.

(2) Levin, E. D.; Simon, B. B.; Conners, C. K. Transdermal Nicotine Treatment of Attention Deficit Hyperactivity Disorder. In *Neuronal Nicotinic Receptors*; Arneric, S. P., Brioni, J. D., Eds.; John Wiley & Sons: New York, 1999; pp 349−357.

(3) Martin-Ruiz, C.; Court, J.; Lee, M.; Piggott, M.; Johnson, M.; Ballard, C.; Kalaria, R.; Perry, R.; Perry, E. Nicotinic Receptors in Dementia of Alzheimer, Lewy Body and Vascular Types. *Acta Neurol. Scand.* **2000**, *102*, 34−41.

(4) Wevers, A.; Burghaus, L.; Moser, N.; Witter, B.; Steinlein, O. K.; Schuetz, U.; Achnitz, B.; Krempel, U.; Nowacki, S.; Pilz, K.; Stoodt, J.; Lindstrom, J.; De Vos, R. A. I.; Steur, E. N. H. J.; Schroeder, H. Expression of Nicotinic Acetylcholine Receptors in Alzheimer's Disease: Postmortem Investigation and Experimental Approaches. *Behav. Brain Res.* **2000**, *113*, 207−215.

(5) Benwell, M. E. M.; Balfour, D. J. K.; Anderson, J. M. Evidence that tobacco smoking increases the density of (−)-[^{3}H]nicotine binding sites in human brain. *J. Neurochem.* **1988**, *50*, 1243−1247.

(6) Steinlein, O. K.; Magnusson, A.; Stoodt, J.; Bertrand, S.; Weiland, S.; Berkovic, S. F.; Nakken, K. O.; Propping, P.; Bertrand, D. An insertion mutation of the CHRNA4 gene in a family with autosomal dominant nocturnal frontal lobe epilepsy. *Hum. Mol. Genet.* **1997**, *6*, 943−947.

(7) Leonard, S.; Adler, L. E.; Benhammou, K.; Berger, R.; Breese, C. R.; Drebing, C.; Gault, J.; Lee, M. J.; Logel, J.; Olincy, A.; Ross, R. G.; Stevens, K.; Sullivan, B.; Vianzon, R.; Virnich, D. E.; Waldo, M.; Walton, K.; Freedman, R. Smoking and mental illness. *Pharmacol. Biochem. Behav.* **2001**, *70*, 561−570.

(8) Holladay, M. W.; Wasicak, J. T.; Lin, N.-H.; He, Y.; Ryther, K. B.; Bannon, A. W.; Buckley, M. J.; Kim, D. J. B.; Decker, M. W.; Anderson, D. J.; Campbell, J. E.; Kuntzweiler, T. A.; Donnelly-Roberts, D. L.; Piattoni-Kaplan, M.; Briggs, C. A.; Williams, M.; Arneric, S. P. Identification and Initial Structure−Activity Relationships of (*R*)-5-(2-Azetidinylmethoxy)-2-chloropyridine (ABT-594), a Potent, Orally Active, Non-Opiate Analgesic Agent Acting via Neuronal Nicotinic Acetylcholine Receptors. *J. Med. Chem.* **1998**, *41*, 407−412.

(9) Lukas, R. J.; Changeux, J. P.; Le Novere, N.; Albuquerque, E. X.; Balfour, D. J. K.; Berg, D. K.; Bertrand, D.; Chiappinelli, V. A.; Clarke, P. B. S.; Collins, A. C.; Dani, J. A.; Grady, S. R.; Kellar, K. J.; Lindstrom, J. M.; Marks, M. J.; Quik, M.; Taylor, P. W.; Wonnacott, S. International Union of Pharmacology. XX. Current status of the nomenclature for nicotinic acetylcholine receptors and their subunits. *Pharmacol. Rev.* **1999**, *51*, 397−401.

(10) Hall, M.; Zerbe, L.; Leonard, S.; Freedman, R. Characterization of [^{3}H]cytisine binding to human brain membrane preparations. *Brain Res.* **1993**, *600*, 127−133.

(11) Sihver, W.; Gillberg, P. G.; Nordberg, A. Laminar distribution of nicotinic receptor subtypes in human cerebral cortex as determined by [^{3}H](−)nicotine, [^{3}H]cytisine and [^{3}H]epibatidine in vitro autoradiography. *Neuroscience* **1998**, *85*, 1121−1133.

(12) Marutle, A.; Warpman, U.; Bogdanovic, N.; Nordberg, A. Regional distribution of subtypes of nicotinic receptors in human brain and effect of aging studied by (±)-[^{3}H]epibatidine. *Brain Res.* **1998**, *801*, 143−149.

(13) Fadda, P.; Martellotta, M. C.; Gessa, G. L.; Fratta, W. Dopamine and opioids interactions in sleep deprivation progress. *Prog. Neuropsychopharmacol. Biol. Psychiatry* **1993**, *17*, 269−278.

(14) Sun, W.; Ginovart, N.; Ko, F.; Seeman, P.; Kapur, S. In vivo evidence for dopamine-mediated internalization of D2-receptors after amphetamine: Differential findings with [^{3}H]raclopride versus [^{3}H]spiperone. *Mol. Pharmacol.* **2003**, *63*, 456−462.

(15) Kessler, R. M.; Sib Ansari, M.; Schmidt, D. E.; de Paulis, T.; Clanton, J. A.; Innis, R.; Al Tikriti, M.; Manning, R. G.; Gillespie, D. High affinity dopamine D2 receptor radioligands. 2. [^{125}I]-epidepride, a potent and specific radioligand for the characterization of striatal and extrastriatal dopamine D2 receptors. *Life Sci.* **1991**, *49*, 617−628.

(16) Pohjalainen, T.; Rinne, J. O.; Nagren, K.; SyvAlahti, E.; Hietala, J. Sex Differences in the Striatal Dopamine D2 Receptor Binding Characteristics in Vivo. *Am. J. Psychiatry* **1998,** *155*, 768−773.

(17) Barnes, J. M.; Barnes, N. M.; Barber, P. C.; Champaneria, S.; Costall, B.; Hornsby, C. D.; Ironside, J. W.; Naylor, R. J. Pharmacological comparison of the sigma recognition site labelled by [^{3}H]haloperidol in human and rat cerebellum. *Naunyn-Schmiedeberg's Arch. Pharmacol.* **1992**, *345*, 197−202.

(18) Sanabria-Bohorquez, S. M.; De Volder, A. G.; Arno, P.; Sibomana, M.; Coppens, A.; Michel, C.; Veraart, C. Decreased benzodiazepine receptor density in the cerebellum of early blind human subjects. *Brain Res.* **2001**, *888*, 203−211.

(19) Horti, A.; Ravert, H. T.; London, E. D.; Dannals, R. F. Synthesis of a Radiotracer for Studying Nicotinic Acetylcholine Receptors: (±)-Exo-2-(2-[^{18}F]fluoro-5-pyridyl-7-azabicyclo[2.2.1]heptane. *J. Labelled Compd. Radiopharm.* **1996**, *38*, 355−365.

(20) Spang, J. E.; Patt, J. T.; Westera, G.; Schubiger, P. A. Comparison of *N*-[^{11}C]methyl-norchloroepibatidine and *N*-[^{11}C]methyl-2-(2-pyridyl)-7-azabicyclo[2.2.1]heptane with *N*-[^{11}C]methyl-epibatidine in small animal PET studies. *Nucl. Med. Biol.* **2000**, *27*, 239−247.

(21) Ding, Y. S.; Gatley, S. J.; Fowler, J. S.; Volkow, N. D.; Aggarwal, D.; Logan, J.; Dewey, S. L.; Liang, F.; Carroll, F. I.; Kuhar, M. J. Mapping nicotinic acetylcholine receptors with PET. *Synapse* **1996**, *24*, 403−407.

(22) Horti, A. G.; Koren, A. O.; Ravert, H. T.; Musachio, J. L.; Mathews, W. B.; London, E. D.; Dannals, R. F. Synthesis of a radiotracer for studying nicotinic acetylcholine receptors: 2-[^{18}F]-fluoro-3-(2(*S*)-azetidinylmethoxy)pyridine (2-[^{18}F]A-85380). *J. Labelled Compd. Radiopharm.* **1998**, *41*, 309−318.

(23) Patt, J. T.; Spang, J. E.; Westera, G.; Buck, A.; Schubiger, P. A. Synthesis and in vivo studies of [C-11]*N*-methylepibatidine: comparison of the stereoisomers. *Nucl. Med. Biol.* **1999**, *26*, 165−173.

(24) Kubinyi, H. The quantitative analysis of structure−activity relationships. In *Burger's Medicinal Chemistry and Drug Discovery*, 6th ed.; Abraham, D. J., Ed.; John Wiley and Sons: New York, 1995; pp 497−571.

(25) Kao Chih-Hao, K.; Waki, A.; Sassaman, M. B.; Jagoda, E. M.; Szajek, L. P.; Ravasi, L.; Shimoji, K.; Eckelman, W. C. Evaluation of [^{76}Br]FBAU 3′,5′-dibenzoate as a lipophilic prodrug for brain imaging. *Nucl. Med. Biol.* **2002**, *29*, 527−535.

(26) Dischino, D. D.; Welch, M. J.; Kilbourn, M. R.; Raichle, M. E. Relationship between lipophilicity and brain extraction of carbon-11-labeled radiopharmaceuticals. *J. Nucl. Med.* **1983**, *24*, 1030−1038.

(27) Welch, M. J.; Chi, D. Y.; Mathias, C. J.; Kilbourn, M. R.; Brodack, J. W.; Katzenellenbogen, J. A. Biodistribution of *N*-alkyl and *N*-fluoroalkyl derivatives of spiroperidol; radiopharmaceuticals for PET studies of dopamine receptors. *Nucl. Med. Biol.* **1986**, *13*, 523−526.

(28) Kessler, R. M.; Ansari, M. S.; de Paulis, T.; Schmidt, D. E.; Clanton, J. A.; Smith, H. E.; Manning, R. G.; Gillespie, D.; Ebert, M. H. High-Affinity Dopamine-D2 Receptor Radioligands. 1. Regional Rat-Brain Distribution of Iodinated Benzamides. *J. Nucl. Med.* **1991**, *32*, 1593−1600.

(29) de Paulis, T. The discovery of epidepride and its analogs as high-affinity radioligands for imaging extrastriatal dopamine D2 receptors in human brain. *Curr. Pharm. Des.* **2003**, *9*, 673−696.

(30) Huang, Y.; Hwang, D. R.; Narendran, R.; Sudo, Y.; Chatterjee, R.; Bae, S. A.; Mawlawi, O.; Kegeles, L. S.; Wilson, A. A.; Kung, H. F.; Laruelle, M. Comparative Evaluation in Nonhuman Primates of Five PET Radiotracers for Imaging the Serotonin Transporters: [^{11}C]McN 5652, [^{11}C]ADAM, [^{11}C]DASB, [^{11}C]-DAPA, and [^{11}C]AFM. *J. Cereb. Blood Flow Metab.* **2002**, *22*, 1377−1398.

(31) Kimes, A. S.; Horti, A. G.; London, E. D.; Chefer, S. I.; Contoreggi, C.; Ernst, M.; Friello, P.; Koren, A. O.; Kurian, V.; Matochik, J. A.; Pavlova, O.; Vaupel, D. B.; Mukhin, A. G. 2-[^{18}F]F-A85380: PET Imaging of Brain Nicotinic Acetylcholine Receptors and Whole Body Distribution in Humans. *FASEB J.* **2003**, *17*, 1331−1333.

(32) Bottlaender, M.; Valette, H.; Roumenov, D.; Dolle, F.; Coulon, C.; Ottaviani, M.; Hinnen, F.; Ricard, M. Biodistribution and radiation dosimetry of [^{18}F]fluoro-A-85380 in healthy volunteers. *J. Nucl. Med.* **2003**, *44*, 596−601.

(33) Kimes, A. S.; Chefer, S. I.; Matochik, J. A.; Pavlova, O. A.; Contoreggi, C. S.; Horti, A. G.; Kurian, V.; Vaupel, B. D.; Friello, P.; Koren, A. O.; Ernst, M.; London, E. D.; Mukhin, A. G. Quantitation of human cerebral nicotinic acetylcholine receptors with 2-[^{18}F]F-A85380 and PET. Presented at the 33rd Annual Meeting of the Society for Neuroscience,, New Orleans, 2003.

(34) Chefer, S. I.; London, E. D.; Koren, A. O.; Pavlova, O. A.; Kurian, V.; Kimes, A. S.; Horti, A. G.; Mukhin, A. G. Graphical Analysis of 2-[^{18}F]FA Binding with Nicotinic Acetylcholine Receptors in Rhesus Monkey Brain. *Synapse* **2003**, *48*, 25−34.

(35) Ichise, M.; Meyer, J. H.; Yonekura, Y. An Introduction to PET and SPECT Neuroreceptor Quantification Models. *J. Nucl. Med.* **2001**, *42*, 755−763.

(36) Lin, N.-H.; He, Y.; Holladay, M. W. 3-Pyridyloxymethyl heterocyclic ether compounds useful as nicotinic cholinergic ligands in controlling chemical synaptic transmission. U.S. Patent 5,-629,325, 1996.

(37) Carroll, F. I.; Lee, J. R.; Navarro, H. A.; Ma, W.; Brieaddy, L. E.; Abraham, P.; Damaj, M. I.; Martin, B. R. Synthesis, Nicotinic Acetylcholine Receptor Binding, and Antinociceptive Properties of 2-exo-2-(2′,3′-Disubstituted 5′-pyridinyl)-7-azabicyclo[2.2.1]-heptanes: Epibatidine Analogs. *J. Med. Chem*. **2002**, *45*, 4755−4761.

(38) Brown, L. L.; Kulkarni, S.; Pavlova, O. A.; Koren, A. O.; Mukhin, A. G.; Newman, A. H.; Horti, A. G. Synthesis and Evaluation of a Novel Series of 2-Chloro-5-((1-methyl-2-(*S*)-pyrrolidinyl)-methoxy-3-(2-(4-pyridinyl)vinyl)pyridine Analogues as Potential Positron Emission Tomography Imaging Agents for Nicotinic Acetylcholine Receptors. *J. Med. Chem*. **2002**, *45*, 2841−2849.

(39) Haino, T.; Yamanaka, Y.; Araki, H.; Fukazawa, Y. Metal-Induced Regulation of Fullerene Complexation with Double-Calix[5]-arene. *Chem. Commun*. **2002**, *5*, 402−403.

(40) Henze, O.; Lehmann, U.; Schlueter, A. D. Synthesis of 5,5′-Disubstituted 2,2-Bipyridines for Modular Chemistry. *Synthesis* **1999**, *4*, 683−687.

(41) Abreo, M. A.; Lin, N. H.; Garvey, D. S.; Gunn, D. E.; Hettinger, A. M.; Wasicak, J. T.; Pavlik, P. A.; Martin, Y. C.; Donnelly-Robert, D. L.; Anderson, D. J.; Sullivan, J. P.; Williams, M.; Arneric, S. P.; Holladay, M. W. Novel 3-Pyridyl Ethers with Subnanomolar Affinity for Central Neuronal Nicotinic Acetylcholine Receptors. *J. Med. Chem*. **1996**, *39*, 817−825.

(42) Horti, A. G.; Scheffel, U.; Kimes, A. S.; Musachio, J. L.; Ravert, H. T.; Mathews, W. B.; Zhan, Y.; Finley, P. A.; London, E. D.; Dannals, R. F. Synthesis and Evaluation of N-[^{11}C]Methylated Analogues of Epibatidine as Tracers for Positron Emission Tomographic Studies of Nicotinic Acetylcholine Receptors. *J. Med. Chem*. **1998**, *41*, 4199−4206.

(43) Rocca, P.; Cochennec, C.; Marsais, F.; Thomas-dit-Dumont, L.; Mallet, M.; Godard, A.; Quéguiner, G. First Metalation of Aryl Iodides: Directed Ortho-Lithiation of Iodopyridines, Halogen-Dance, and Application to Synthesis. *J. Org. Chem*. **1993**, *58*, 7832−7838.

(44) Estel, L.; Marsais, F.; Quéguiner, G. Metalation/$S_{RN}1$ Coupling in Heterocyclic Synthesis. A Convenient Methodology for Ring Functionalization. *J. Org. Chem*. **1988**, *53*, 2740−2744.

(45) Marsais, F.; Pineau, P.; Nivolliers, F.; Mallet, M.; Turck, A.; Godard, A.; Quéguiner, G. A New Convergent Route to 1-Substitited Ellipticines. *J. Org. Chem*. **1992**, *57*, 565−573.

(46) Mukhin, A. G.; Gundisch, D.; Horti, A. G.; Koren, A. O.; Tamagnan, G.; Kimes, A. S.; Chambers, J.; Vaupel, D. B.; King, S. L.; Picciotto, M. R.; Innis, R. B.; London, E. D. 5-Iodo-A-85380, an $\alpha4\beta2$ Subtype-Selective Ligand for Nicotinic Acetylcholine Receptors. *Mol. Pharmacol*. **2000**, *57*, 642−649.

(47) Quik, M.; Polonskaya, Y.; Kulak, J. M.; Mclntosh, J. M. Vulnerability of ^{125}I-α-Conotoxin MII Binding Sites to Nigrostriatal Damage in Monkey. *J. Neurosci*. **2001**, *21*, 5494−5500.

(48) Whiteaker, P.; Mcintosh, J. M.; Luo, S.; Collins, A. C.; Marks, M. J. ^{125}I-α-Conotoxin MII Identifies a Novel Nicotinic Acetylcholine Receptor Population in Mouse Brain. *Mol. Pharmacol*. **2000**, *57*, 913−925.

(49) *ACD/LogD Suite*; Advanced Chemistry Development Inc.: Toronto, Canada.

(50) Wilson, A. A.; Jin, L.; Garcia, A.; DaSilva, J. N.; Houle, S. An admonition when measuring the lipophilicity of radiotracers using counting techniques. *Appl. Radiat. Isot*. **2001**, *54*, 203−208.

(51) Hamacher, K.; Coenen, H. H.; Stoecklin, G. Efficient stereospecific synthesis of no-carrier-added 2-[^{18}F]-fluoro-2-deoxy-D-glucose using aminopolyether supported nucleophilic substitution. *J. Nucl. Med*. **1986**, *27*, 235−238.

(52) Chefer, S. I.; Horti, A. G.; Koren, A. O.; Gundisch, D.; Links, J. M.; Kurian, V.; Dannals, R. F.; Mukhin, A. G.; London, E. D. 2-[^{18}F]F-A-85380: A PET Radioligand for $\alpha_4\beta_2$ Nicotinic Acetylcholine Receptors. *NeuroReport* **1999**, *10*, 2715−2721.

(53) Logan, J. Graphical Analysis of PET Data Applied to Reversible and Irreversible Tracers. *Nucl. Med. Biol*. **2000**, *27*, 661−670.

(54) Chefer, S. I.; Pavlova, O. A.; Zhang, Y.; Vaupel, D. B.; Kimes, A. S.; Kurian, V.; Horti, A. G.; Mukhin, A. G. NIDA 522189 and NIDA 522131: New Promising Radioligands for PET Imaging Extrathalamic Nicotinic Receptors. *J. Labelled Compd. Radiopharm*. **2003**, *46*, S63.

(55) Sheridan, R. P.; Nilakantan, R.; Dixon, J. S.; Venkataraghavan, R. The Ensemble Approach to Distance Geometry: Application to the Nicotinic Pharmacophore. *J. Med. Chem*. **1986**, *29*, 899−906.

(56) Glennon, R. A.; Dukat, M. Central nicotinic receptor ligands and pharmacophores. *Pharm. Acta Helv*. **2000**, *74*, 103−114.

(57) Koren, A. O.; Horti, A. G.; Mukhin, A. G.; Gundisch, D.; Kimes, A. S.; Dannals, R. F.; London, E. D. 2-, 5-, and 6-Halo-3-(2(*S*)-azetidinylmethoxy)pyridines: Synthesis, Affinity for Nicotinic Acetylcholine Receptors, and Molecular Modeling. *J. Med. Chem*. **1998**, *41*, 3690−3698.

(58) Brejc, K.; van Dijk, W. J.; Klaassen, R. V.; Schuurmans, M.; van der Oost, J.; Smit, A. B.; Sixma, L. K. Crystal structure of an ACh-binding protein reveals the ligand-binding domain of nicotinic receptors. *Nature* **2001**, *411*, 269−276.

(59) Glennon, R.; Dukat, M. Nicotinic Cholinergic Receptor Pharmacophores. In *Neuronal Nicotinic Receptors*; Arneric, S. P., Brioni, J. D., Eds.; John Wiley & Sons: New York, 1999; pp 271−284.

(60) Lin, N.-H.; Li, Y.; He, Y.; Holladay, M. W.; Kuntzweiler, T. A.; Anderson, D. J.; Campbell, J. E.; Arneric, S. P. Synthesis and Structure−Activity Relationships of 5-Substituted Pyridine Analogues of 3-[2-((*S*)-Pyrrolidinyl)methoxy]pyridine, A-84543: A Potent Nicotinic Receptor Ligand. *Bioorg. Med. Chem. Lett*. **2001**, *11*, 631−633.

JM030432V